UNIVERSITÀ DEGLI STUDI DI PADOVA

Dipartimento di Ingegneria dell'Informazione

Corso di Laurea in Ingegneria Informatica

TESI DI LAUREA

Analisi e progettazione di filtri IIR derivativi per segnali quantizzati

Analysis and design of IIR differentiator for quantized signals

RELATORE: Prof. Sergio Congiu

RELATORE: Prof. Richard Kavanagh

LAUREANDO: Giacomo Portolan

A.A. 2011-2012

Vola solo chi osa farlo

Luis Sepulveda

Abstract

The IIR differentiators are nowadays largely studied for different kind of uses, such as in Sigma-Delta modulation and data compression. However, estimation of velocity, based on quantized signals (i.e. provided by incremental optical encoder) and using differentiators is still a challenge, since the quantization process has an associated error that shows non-linearity properties.

The thesis provides a complete framework on IIR digital differentiators when used for velocity estimation with quantized position signals as input: the most important is a procedure that allows everyone to calculate the mean square error at the output of the filter when the autocorrelation of the input error is known. This achievement can be also applied to every kind of IIR filter giving to it a wide range of applications. Moreover, a comparison between the real error and the white noise approximation has been made, and also a new approximation, based on the worst case, has been developed. Last, a full spectral analysis of the filters and signals has been provided.

Most of the results above have been provided and tested for the constant rate case, in order to optimize the IIR differentiator for system with low frequencies rate of change.

Acknowledgements

I would like to thank my mom and my dad because without them I would probably not be the man that I am now. They unconditionally gave me all their trust, support, patience, love and advices in these years that I spent in Padova, without asking for reasons or results, but with a genuine interest in my life. I also want to dedicate this thesis to them, because they were always present for me during my Erasmus experience in Ireland.

My "partners" in the developing of this thesis were the Irish supervisor, Prof. Richard Kavanagh, and the Italian supervisor, Prof. Sergio Congiu. I would like to thank them a lot for all the time, help and advices that they gave and dedicated to me during the last six month. Moreover, I would like to thank Prof. Leonardo Giudicotti because without his efforts and passion I would not be able to develop my thesis abroad.

A huge thanks to Lucia! She had a lot of patience during all these years and I hope she would have enough of that also for the future! We have spent together the experience of the University, sharing feelings, experiences, friends and much more besides and all these elements have allowed us to grow as single person and also as couple. I hope we could continue on this road together for a long time.

Thank you Giulia, because the distance that has separated us physically, has also changed our relationship: we are no more "cane e gatto", we are friends now. I

would also thank you (with some years of delay) for the babysitting that you made me during the high school!

Thank you Dario, Martina, Elisa, Lorenzo and all the other students which shared with me happy and bad times at DEI! I would be bored out of my mind without anyone of you!

Can I forget my second family? Of course not! Lucio, Federico, Andrea, Matteo, Matteo, Alberto, Clive, all the fishes and other strange animals of Liberty Street and why not…also Diletta! Now, together, we should thanks Magarottos for the great apartment!

Thanks to all the teammates that I met during my years at Albignasego and Noventa because everyone of you has been part of my daily life and you will always be in my memories.

Cheers to my third family of, again, Liberty Street (Ireland in this case)!

Thanks to all my friends of Pordernone, Padova and Cork that I have not mentioned here but, believe me, I will drink to you!

Contents

List of figures

List of Abbreviation

DSP: Digital Signal Processing

DSP: Digital Signal Processor

FPGA: Field-Programmable Gate Array

ADC: Analogue to Digital Converter

DAC: Digital to Analogue Converter

LTI: Linear and Time Invariant

FIR: Finite Impulse Response

IIR: Infinite Impulse Response

MSE: Mean Square Error

DFT: Discrete Fourier Transform

Introduction

This thesis is about the analysis and design of IIR differentiators for quantized signals, in particular for the velocity estimation of a rotating shaft. An encoder provides the input signal (position information of the system in motion), and the filter estimates the actual velocity: most of the results are focused on the constant rate case, where the input signal is a quantized ramp and the expected output is the slope of that ramp.

The main aim of the project is to infer a closed form solution for the mean square error at the output of the differentiator when a quantized input is filtered. The results are functions of the fractional value of the rate and the coefficients of the filter. Moreover, this thesis will present an innovative process, which allows the reader to design IIR differentiators with optimal attenuation of the quantization noise (especially in the constant rate case). Then a comparison will be made between the results just achieved with the common assumption that the quantization noise could be modeled as white noise. As expected, in most cases such approximation is very poor in most of the cases and, in order to provide a better instrument, a new approximation based on the worst case will be proposed. Last, a spectral analysis of signals and filters will be presented in detail.

The analysis and design of IIR digital differentiators in connection with quantized signals, such as in digital tachometry, is innovative in the field of digital signal processing and some of the results achieved represent a future state of the art in this particular field. On the other hand, some general formulae and process have been achieved, which could be used in every field that involves IIR filters.

The first chapter of this work provides the general information that will be largely used in the remainder of the thesis:

- Quantization, quantization error and the white noise assumption; most of the results are based on previous work on FIR filters.
- A quick review on digital signals, filters and their properties.
- Almost periodic signals and Bohr spectrum: they provide instruments that allow the work on the project to be simplified.
- Digital tachometry and the constant rate case: is the main motivation for the project to be developed because most of the results will be applied in this field.

Although this knowledge will be largely used in the other chapters, since they are basic and very general, a wise reader could feel free to skip them and start reading from the following and more interesting chapters, which present the actual work done.

The second chapter presents the results from the analysis of the first order IIR digital differentiator: it begins with an introduction of the filter and then shows the formulae and experimental results achieved on the mean square error (MSE), white noise approximation, worst case approximation and spectral analysis. The outcomes are presented in a general fashion and, when tested, the input is provided by an incremental optical encoder of a constant rate rotating shaft. In both cases the first order IIR digital differentiators does not provide a sufficient general case for the analysis so, in the following chapter, the second order will be taken into account, which adds some properties to the work.

The third chapter has the same outline as the previous one; however, it has been developed using a second order IIR digital filter: the distinction between the two is essential because some analysis challenges and design issues are not presented in the first order, since its only coefficient is the feedback coefficient. Using the second order IIR differentiator the new challenges involve a more elaborated recurrence equation, the choice of the filter coefficients (very important in order to achieve a good attenuation of the quantization noise) and a higher complexity in the processes used for inferring the formulae and other results.

The analysis and the design of IIR differentiators are then presented for filters of general order. This chapter has the same outline of the previous two and it merges the considerations made in a general way. The process to derive the MSE at the output of the filter deserves particular attention because, with slightly changes in the deriving method, it

can be applied to an IIR filter without restrictions on the filter coefficients (i.e. a differentiator), and it allows calculating the MSE at the output of every IIR filter when the autocorrelation of the input error is known.

Then, some projects are presented, which can be developed as continuation of this thesis in various directions, such as an implementation of the work done on a physical digital tachometer, a detailed comparison between FIR and IIR differentiators and the use of the estimated velocity in a close loop control system.

1 Relevant theory and state of the art

Nowadays digital signals have a wide spectrum of uses and the number of advantages they involve grows hand by hand with the computational power available everywhere.

Digital Signal Processing (DSP) offers various solutions to handle this kind of signals. The techniques or algorithms known are usually cheaper and easier to implement respect their analogue counterpart, especially when the signal is inherent discrete. Moreover, they are scalable, feature that simplify the design when some specific requirements have to be satisfied: simple and slow speed signals can be handled by many embedded systems or other more general solutions like Field-Programmable Gate Array (FPGA), real time processing of very complex or multiple signals can be executed by huge and very expensive supercomputers.

An example of Digital Signal Processor (DSP) is given in the figure below:

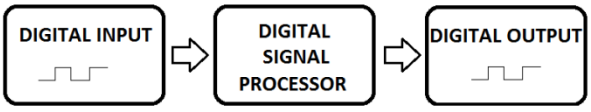

Figure 1.1: Scheme of an implementation of Digital Signal Processing.

For all the reasons explained above, sometimes, is more convenient to convert analogue signals into their sampled version rather than design analogue techniques or devices that process them. To accomplish this task are usually used samplers that, given a continuous time signal, provide a discrete time version of it at a constant sampling rate (since sampling is not matter of interest in the project see sections 5.2 and 5.3 of [24] or more specific

papers for further information). If the overall process after the DSP needs analogue signal again, an interpolator must be inserted after the DSP in order to recreate a continuous time waveform.

An example of the process is shown in the figure below:

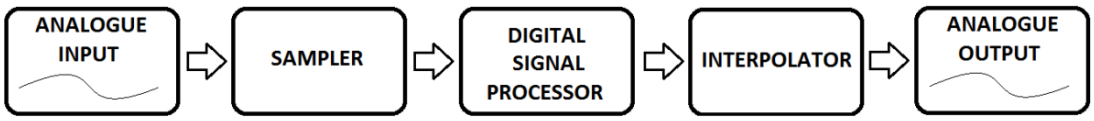

Figure 1.2: Scheme of an implementation of Digital Signal Processing of time sampled analogue signals.

In other cases the DSP can process only signals which are discrete in both time and amplitude. To provide this kind of input at the system, a slightly adjustment has to be done at the scheme in Figure 1.2, where the sampler needs to be replaced by an Analogue to Digital Converter (ADC) and the Interpolator by a Digital to Analogue Converter (DAC).

The improved scheme is depicted in the figure below:

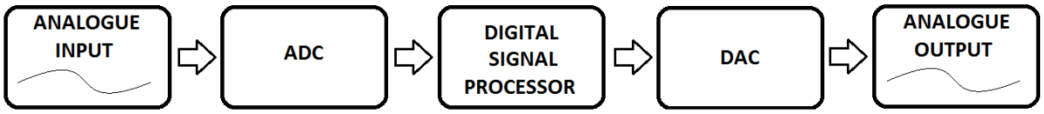

Figure 1.3: Scheme of an implementation of Digital Signal Processing of analogue signals discretized in both time and amplitude.

If no additive noise is inserted in the model (normal noise or specific dithering), the two main differences between the systems described by Figure 1.2 and Figure 1.3 concern the quality of the signal at the output of the DSP, often express in terms of mean square error, and the capability of rebuild an analogue output signal that exactly matches the expectations (see Sections 5.10 and 5.11 of [24]). Both differences rely in the presence of a non-linear transformation inside the ADC: the ADC is composed by a sampler, which performs the time discretization, and an encoder, which performs the amplitude discretization (see sections 5.8 and 5.9 of [24] for further information). The encoder is object of interest in this work because it could be implemented by a quantizer, which is the element that introduces the non-linearity.

The sampling process is generally well understood and a lot of efforts have been made in order to achieve better and better results on this filed. On the other hand the quantization process, due to his non-linearity, is more complex to analyse and handle in application such

as filter design or modulation. The approximations of the quantization error proposed until now works well only in some specific cases, because if used in a general way they introduce in the results achieved a very poor quality. An interesting comparison between these two subjects has been developed in [8], where the analogous of the sampling theorem has been proved for the quantization.

As briefly described above, the thesis is focused on the estimation of the error introduced in the system by the quantizer and how to attenuate it. However, to achieve these results more theoretical and practical knowledge are needed. In the following sections will be presented the quantization and its properties, digital signals and filters as practical application of the DSP, Fourier transform and Bohr spectrum for the frequency domain analysis and tachometers as practical applications of the project.

1.1 Quantization

The early works on quantization began in the first years of the 19th Century. Nevertheless, the first high-resolution analysis on this filed was made by Bennett in 1948 (see [2]).

The simplest way to describe it is to think about the rounding function, $\lfloor \cdot \rfloor$ (floor) or $\lceil \cdot \rceil$ (ceiling), commonly used in various fields that involve mathematical analysis. Some definition of quantization are given in [8], as a map between a larger set/alphabet of input (even infinite) into a smaller one of output, or, as stated in [9], as the division of a quantity into a discrete number of parts, often assumed to be integral multiples of a common quantity.

A basic assumption will be made on quantization in order to continue its presentation. According on the kind of input there are two type of quantization: scalar and vector. In the remaining of the work only scalar quantization will be analysed according to the main purpose of the project.

A more general and formal definition of quantization is also given in [9]:

"...a set of intervals or cells $S = \{S_i; i \in \mathrm{I}\}$, ..., together with a set of reproduction values or points or levels $C = \{y_i; i \in \mathrm{I}\}$, so the overall quantization function $q(\cdot)$ is defined by $q(x) = y_i \; for \; x \in S_i$, which can be expressed concisely as

$$q(x) = \sum_i y_i 1_{S_i}(x)$$

where the indicator function $1_{S_i}(x)$ is 1 if $x \in S_i$ and 0 otherwise. For this definition to make sense we assume that S is a partition of the real line (so cells are disjoint and exhaustive)...".

The quantization can also be uniform or nonuniform according on the width of the cells (also named bins): the first has cells equally spaced while the latter has no precise constrains on cells' width. Particular attention has to be paid when the cells are equally spaced but they are in a finite number: this is still uniform quantization but is affected by two different noises as we will see moreover.

In agreement with [4] only uniform quantization is considered because "...a priori there is no knowledge of the statistical behaviour of the input signal and hence there is no way to optimize the quantizer levels...".

The relevant theory on quantization necessary to understand the main aims and goals of the project has been briefly introduced and will be exhaustively presented soon, but for a wider and deeper discussion on quantization, such as history, more basic concept, high resolution theory and quantization techniques, see [9].

1.1.1 Quantizer

The (uniform) quantizer is the actuator of the quantization function, which has been previously designed in order to match some specific requirements of the project. It takes as an input some continuous quantities and it provides as an output some codes, which are given by the label of the closest cell to the input. For the purpose of the project will be considered every real number ($\mathbb{R}$) as possible domain of the input and will be labelled each cell or bin of the quantizer with the number in the middle of it (e.g. with a bin defined on $[a, b)$ its label will be the number $(b + a)/2$).

The various definitions of quantizer are similar in various literatures as [1], [2], [4], [6], [9] and the following one is a merging of all of them. A quantizer with $N < \infty$ bins of width Δ (except for the leftmost and rightmost bins which in this case have semi-infinite width) is given by the quantization rule $q(\cdot)$:

$$q(x) = \begin{cases} \left(\frac{N}{2} - \frac{1}{2}\right)\Delta & when \quad \left(\frac{N}{2} - 1\right)\Delta \leq x \\ \left(k - \frac{1}{2}\right)\Delta & when \quad (k-1)\Delta \leq x < k\Delta; \quad k = \left(-\frac{N}{2} + 2\right), \dots, \left(\frac{N}{2} - 1\right) \\ \left(-\frac{N}{2} + \frac{1}{2}\right)\Delta & when \quad x < \left(-\frac{N}{2} + 1\right)\Delta \end{cases} \tag{1.1}$$

If the number of levels N of the quantizer is infinite the quantization rule can be simplified as shown in (1.2) because all its cells have equal width.

$$q(x) = \left(k - \frac{1}{2}\right)\Delta \qquad when \qquad (k-1)\Delta \leq x < k\Delta \tag{1.2}$$

The special case of N = 8 is shown below:

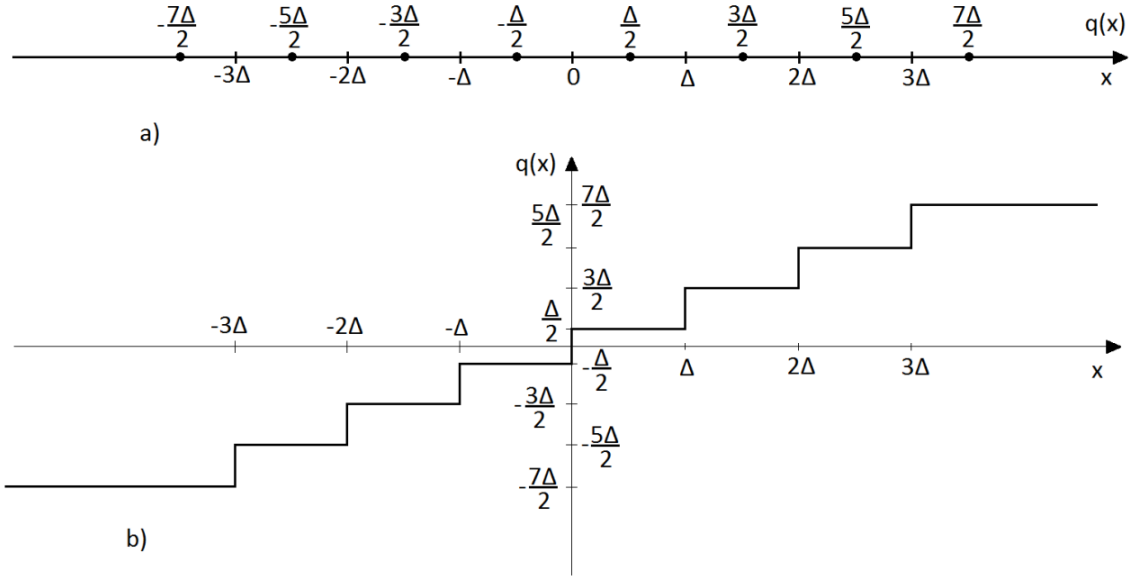

Figure 1.4: Example 1-D (a) and 2-D (b) of quantizer the q(x) with N = 8. It easy to see that the lesftmost and the rightmost cells have semi-infinite width.

For the purpose of the project will be considered a quantizer with $N = \infty$ number of levels and bins with unity width, therefore, it is basically the rounding function from the Real Numbers ($\mathbb{R}$) to the Integers($\mathbb{Z}$). As described in Section 2.2 of [1], the quantization function of this special case can have three different representations but, despite the exteriors differences, they have equivalent behaviour in the mathematical analysis. The following quantizer has been used in the project due to its zero mean in the error domain (see 1.1.2) and its slightly simpler Fourier series representation:

$$q(x) = \lfloor x \rfloor + \frac{1}{2} \qquad x \in \mathbb{R} \tag{1.3}$$

The graphical representation of (1.3) is depicted in Figure 1.5.

Will be essential for the further analysis to introduce a useful notation adopted by first in [4] and then in [1] in order to simplify the formulae and make instantly clear the relations between input and output: every real number r can be uniquely written in the form

$r = \lfloor r \rfloor + \langle r \rangle$, where $\lfloor r \rfloor$ is the greatest integer less than or equal to r and $0 \leq \langle r \rangle < 1$ is the fractional part of r (or $r \ mod \ 1$). Now (1.3) can be rewritten as:

$$q(x) = x + \frac{1}{2} - \langle x \rangle \qquad\qquad x \in \mathbb{R} \tag{1.4}$$

As mentioned above, the quantizer is a source of error in the system, due to the approximation in rounding the input, and this behaviour will the topic of the following section.

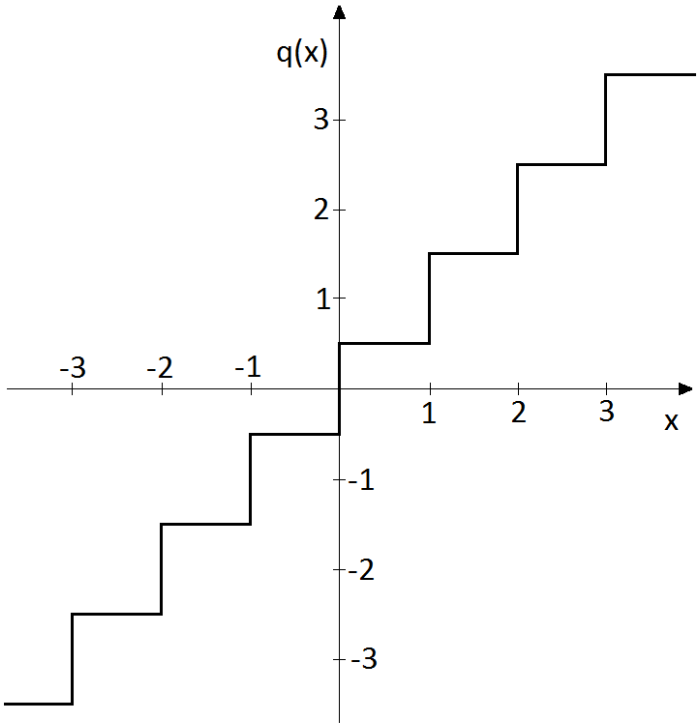

Figure 1.5: Effective quantizer $q(x)$ used in the project. $N = \infty$ and $\Delta = 1$

1.1.2 Quantization error

The nonlinearity property of the quantizer makes it a noisy component. If the quantizer is provided with an infinite number of bins, the only error that affects the output is named granular noise or granular distortion and its formula, according to (1.2), is given by:

$$e(x) = \frac{\varepsilon(x)}{\Delta} = \frac{x - q(x)}{\Delta} = \frac{x}{\Delta} - k + \frac{1}{2} = \frac{x}{\Delta} - (k-1) + \frac{1}{2}$$
$$when \quad k - 1 \leq \frac{x}{\Delta} < k; \quad k = \left(-\frac{N}{2} + 2\right), \dots, \left(\frac{N}{2} - 1\right) \tag{1.5}$$

On the other hand, if the quantizer has a number of levels $N < \infty$, the leftmost and the rightmost bins have semi-infinite dimension. When the absolute value of the input is bigger

than $N/2$, so it lies in one of the two most far bins, the quantizer is in the overload region where the granular noise is known as overload noise or overload distortion. The most important property of such noise is that it is unbounded. The quantization error formula for this kind of quantizer, using (1.1), is given by:

$$e(x) = \frac{\varepsilon(x)}{\Delta} = \begin{cases} \frac{x}{\Delta} - \left(\frac{N}{2} - 1\right) - \frac{1}{2} & when \quad \frac{N}{2} - 1 \leq \frac{x}{\Delta} \\ \frac{x}{\Delta} - (k-1) - \frac{1}{2} & when \quad k - 1 \leq \frac{x}{\Delta} < k; \quad k = \left(-\frac{N}{2} + 2\right), \ldots, \left(\frac{N}{2} - 1\right) \\ \frac{x}{\Delta} - \left(-\frac{N}{2} + 1\right) - \frac{1}{2} & when \quad \frac{x}{\Delta} < -\frac{N}{2} + 1 \end{cases} \tag{1.6}$$

Figure 1.6 shows one case with $N < \infty$ (in particular $N = 6$), and is easy to see that the quantization error is unbounded in the rightmost and leftmost bins.

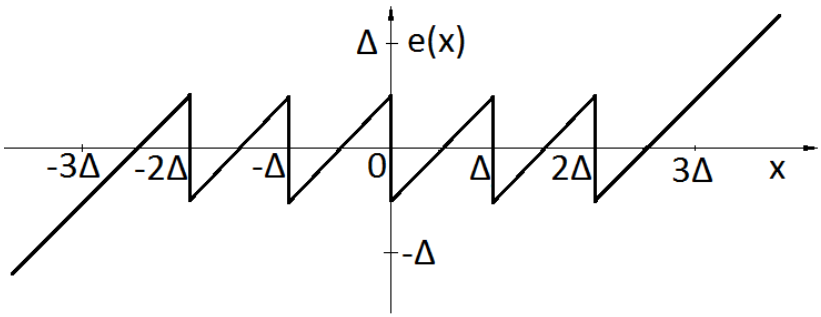

Figure 1.6: Quantization error $e(x)$ of a quantizer with $N = 6$. See that if $|x| > N\Delta/2$ the error grows indefinitely.

In order to avoid that the input signal assumes values of the overload region, it is usually inserted a pre-quantizer filter that rescales the input or bound it in various way so, the only noise added by the quantizer is the granular one.

As mentioned in Section1.1.1, the project adopts (due to practical aspects that will be described in Section 1.4) a quantizer with $N = \infty$ and unity bin's width, so (1.5) has been modified using (1.4). In this practical case the quantization error is given by:

$$e(x) = x - q(x) = \langle x \rangle - \frac{1}{2} \qquad x \in \mathbb{R} \tag{1.7}$$

Since $\langle x \rangle$ is bounded in the interval $[0,1[$, the error $e(x)$ has $\left[-\frac{1}{2}, \frac{1}{2}\right[$ as domain. Figure 1.7 is the graphical representation of (1.7) and, comparing it with Figure 1.6, can be seen that it has not overload region and it is periodic.

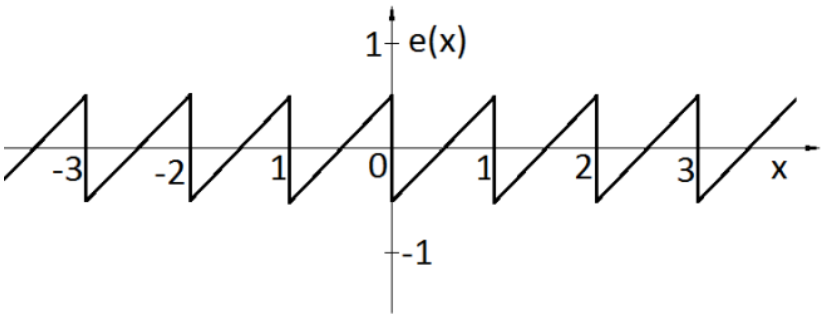

Figure 1.7: Quantization error of project's quantizer. $\Delta = 1$ and since $N = \infty$ there is no overload region.

An interesting property of (1.7) is that it has zero mean when the input is uniformly distributed. This assumption is fundamental and will be used in Section 1.1.3.

From (1.7) it is not easy to see what in Figure 1.7 could be almost taken for granted: the error function, when no overload distortion occurs, is a periodic function. This feature will be useful hereinafter in Section 1.3, where the spectral analysis will be developed.

1.1.3 Assumption as white noise

Since the first analysis of quantized signals and the non-linearity of the quantization function, a lot of efforts had been made to model the quantization error, in order to provide a trustworthy and simple-to-use approximation for error analysis of various systems.

At the beginning, the quantization error was modelled as a signal-independent, uniformly distributed on $\left[-\frac{\Delta}{2}, \frac{\Delta}{2}\right[$, uncorrelated additive noise. This kind of approximation linearizes the system but is not valid in all circumstances (especially when the input signal of the quantizer has a strong autocorrelation, e.g. the constant rate case) and in some cases could lead to very poor results.

When Bennett introduced the high-resolution analysis of quantization [2], he provided constrains under which the white noise approximation can be safely used as quantization error model (additional information can also be found in [3], [4] and [5]). These conditions are the following:

1) The quantizer does not overload
2) The quantizer has a large numbers of levels
3) The bin width or distance between the levels is small
4) The probability distribution of pair of input samples is given by a smooth probability density function

Since Bennett's conditions are not satisfied by general signals (in various ways), another approach used to model quantization error is to force the input to satisfy aforesaid constrains using dithering (see [1], [4], [6], [10] for further information and practical applications). This process allows the designer to use the white noise approximation in the system modelling if he adds a dither (random process independent from the input) at the input signal previously the quantization. Despite this method could lead to good approximation of the noise in the system, it does not provide and exact solution at the problem via a closed form formula.

Approximation seems to be the simplest and most analysed way to model the quantization error. However, one of the main aims of the project is to find a closed form solutions at various problems that involve quantizer (e.g. [1], [7], [10], [12] and [23]). Moreover, in the remainder of the thesis, will be made a comparison between the inferred closed form solution and the white noise approximation and a quantization noise approximation based on the worst case will be proposed, in order to provide guarantees on the MSE boundaries(e.g. if used in system control and feedback loop).

1.2 Digital Filtering

The common implementation of the DSP of Figure 1.1, Figure 1.2 and Figure 1.3 is made by digital filters. In the remainder of this section will be explained some notions on signals theory, what a digital filter is and some of its important properties that has been used in the project (for a complete coverage on digital filter and signals see [24], [25]).

1.2.1 Signals

This section will introduce some important aspects on signals theory as correlation and cross-correlation for almost stationary signals and a way to measure errors on signals.

As stated in [4], Chapter 2 of [24] and Section 2.4 of [1], a signal or stochastic process x(n) can be considered pseudo-stationary or almost-stationary or quasi-stationary if:

- $E\{x(n)\} \leq C \qquad \forall n$
- $|E\{x(n)x(k)\}| \leq C \qquad \forall n, k$

Under these circumstances if (1.18) exists for each value of r, then the limit is named autocorrelation of x(n) and is defined as $R_x(r)$.

$$\lim_{N\to\infty}\frac{1}{N}\sum_{n=1}^{N}E\{x(n)x(n+r)} \tag{1.8}$$

The same reasoning can be applied at the cross-correlation of two quasi-stationary signals x(n) and u(n) , named $R_{xu}(r)$:

$$R_{xu}(r)=\lim_{N\to\infty}\frac{1}{N}\sum_{n=1}^{N}E\{x(n)u(n+r) \qquad \forall r \tag{1.9}$$

A topic connected to the correlation is the signal error measurement. In the project is used the mean square error (MSE) as estimation of the difference between real and simulated signals or between continuous and quantized signals. As described in [9], the MSE is obtained as squared of the difference between a signal and its expectation. For the signal $x(n)$ with mean m_x is given by:

$$MSE_x=\lim_{N\to\infty}\frac{1}{N}\sum_{n=1}^{N}(x(n)-m_x)^2 \tag{1.10}$$

Another point of view for the MSE is to consider it as the average power of the signal represented by the error between $x(n)$ and its average. In this case is possible to bond the autocorrelation and the MSE: considering the signal $e(n)=x(n)-m_x$ it is easy to understand that $MSE_e=R_e(0)$. This relation will be very useful for the aim of the project and both labels will be used in the remainder of the thesis even if they point the same measure.

An error signal provided as an output of a filter has different MSE or autocorrelation according to the input error signal. Åström, Juri and Agniel developed an efficient algorithm for computing MSE_e or equivalently $R_e(r)$ when $r=0$ (see Appendix 2C of [24]) when the input MSE is given: the numerator and the denominator of the filter are given respectively by:

$$C(z)=c_0z^n+c_1z^{n-1}+\cdots+c_n \qquad A(z)=a_0z^n+a_1z^{n-1}+\cdots+a_n$$

Let $a_i^n=a_i$ and $c_i^n=c_i$ and define a_i^k and c_i^k recursively by:

$$a_i^{n-k}=\frac{a_0^{n-k+1}a_i^{n-k+1}-a_{n-k+1}^{n-k+1}a_{n-k+1-i}^{n-k+1}}{a_0^{n-k+1}}$$

$$c_i^{n-k}=\frac{a_0^{n-k+1}c_i^{n-k+1}-c_{n-k+1}^{n-k+1}a_{n-k+1-i}^{n-k+1}}{a_0^{n-k+1}}$$

$$i = 0,1, \dots, n-k \qquad k = 1,2, \dots, n$$

Then given the MSE of the input, named $R_i(0)$, the MSE at the output of the filter, labelled with $R_o(0)$, is given by:

$$R_o(0) = \frac{R_i(0)}{a_0} \sum_{\mathrm{k}=0}^{\mathrm{n}} \frac{\left(\mathrm{c_k^k}\right)^2}{\mathrm{a_0^k}}$$

1.2.2 Filters

A digital filter, named $h(n)$ in the time domain or $H(z)$ in the Z domain, is a system that performs a known mathematical function on a discrete time signal, named $x(n)$ or $X(z)$, in order to produce in the output a desired signal, named $y(n)$ or $Y(z)$. Linear Time Invariant (LTI) and stable digital filter will be only considered in the remainder of the thesis.

Digital filters are completely described by their differential equation that is given by:

$$\sum_{k=0}^{N} a_k y(n-k) = \sum_{k=0}^{M} b_k x(n-k) \tag{1.11}$$

Or by their transfer function or frequency response that are given respectively by:

$$H(z) = \frac{\sum_{k=0}^{M} b_k z^{-k}}{\sum_{k=0}^{N} a_k z^{-k}} \tag{1.12}$$

$$H\left(e^{j\omega}\right) = \frac{\sum_{k=0}^{M} b_k e^{-j\omega k}}{\sum_{k=0}^{N} a_k e^{-j\omega k}} \tag{1.13}$$

Or by their impulse response that is given by:

$$h(n) = \alpha_k \delta(k) \qquad\qquad k \in \mathbb{Z} \tag{1.14}$$

The transfer function of a filter is a fraction of polynomials that have z^{-1} as variable. The roots of the numerators are the zeros of the filter, usually indicated by a circle in the complex plane, while the roots of the denominator are the poles of the filter, labelled by an x in the complex plane. Zeros and poles belong to the complex numbers since the roots of a polynomial are not always real and this means that they can be represented by real-imaginary parts, $a + jb$, or by polar representation $re^{j\theta}$. In the latter, θ will be named phase angle of the zero or pole. Figure 1.8 shows a zero-pole layout. As mentioned above, will be considered only stable filters which, in terms of zero-pole of a filter, mean that all their poles MUST have an absolute value less than the unity (they must be inside the unity circle). On the other hand the zeros could assume every complex value.

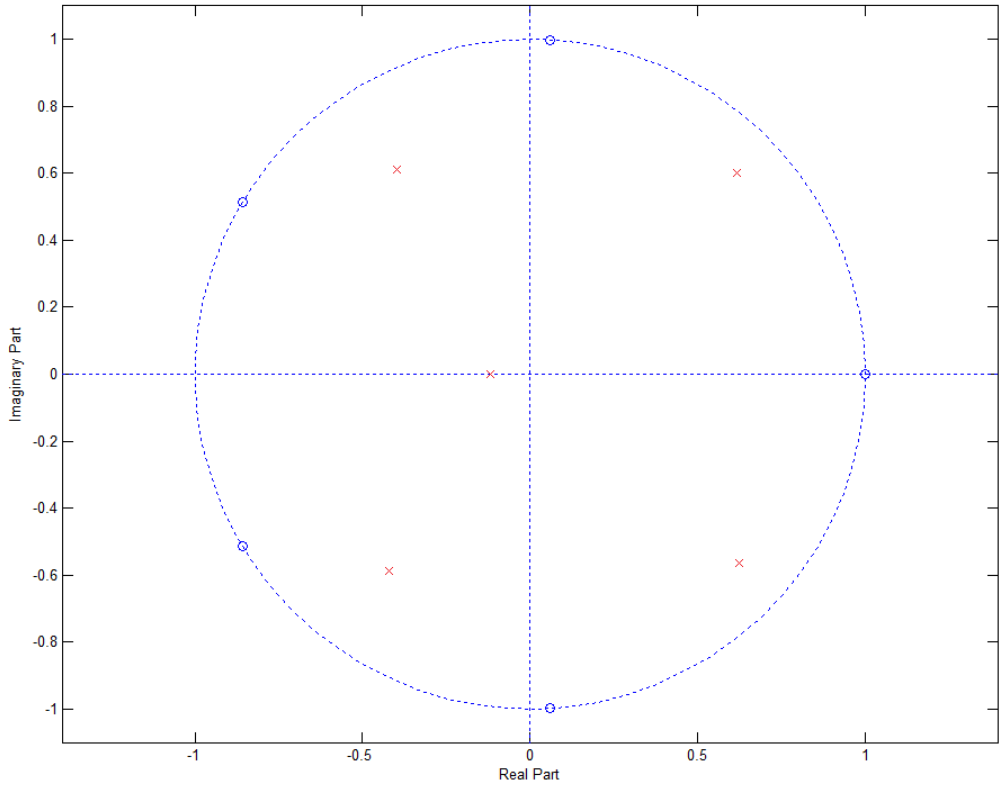

Figure 1.8: Example of zero-pole layout of a stable filter. The ° are the zeros and the × are the poles. For the sake of clarity is depicted also the unity circle.

When a digital filter receives an input signal $x(n)$, it behaves in two different ways while it is computing the output signal $y(n)$: since it starts process $x(n)$ until a certain period of time, which depends on the zeros-poles layout but mostly influenced by the poles, the filter is in the transient state. After that, the filter enters the steady state, in which the initial condition of the system has no further influence. In the remainder of the work, due to practical aspects of the project, the initial transient phase of the system will be neglected.

The common classification for digital filters is in two main categories according to the length of the impulse response: Finite Impulse Response (FIR) and Infinite Impulse Response (IIR).

The first can be equally specified by (1.11) with $N = 0$, by (1.12) or (1.13) with a unity denominator or by (1.14) with a finite numbers of terms α_k different from zero (or $\alpha_k = 0 \; \forall N_1 < k < N_2$ with both N_1, N_2 finite). In (1.11), M specifies the order of the FIR filter which is always stable because it has M poles in the origin (so inside the unity circle).

The latter is more general and it can be described by one of the four methods above without restriction (except for the stability condition). In this case the maximum between N and M

represents the order of the IIR filter. The stability of the IIR filters needs always to be checked during the design of the component, because the poles of the filter could have absolute value higher than the unity.

The differentiator filter is a particular kind of FIR or IIR filter which provides as an output a signal proportional to the time derivative of the input.

Implementation of differentiator, using FIR filter, can be made following Section 4.4.3 of [25] in order to obtain a linear phase filters. As it will turn out in Section 1.2.3, filters with linear phase (or constant group delay) are more useful. Then to design a proper differentiator are required two more constrains. Given the FIR filter transfer function $H(z) = \sum_{k=0}^{M} b_k z^{-k}$ the filter must satisfy the following equations:

$$\sum_{k=0}^{M} b_k = 0$$

$$\sum_{k=0}^{M} k b_k = -1$$

The first (implicit if the filter has a linear phase) imposes zero gain at constant input while the second provides the slope of the input ramp at the output of the filter when a ramp in processed (see [1], [12], [13], [14] for further information). Digital FIR differentiator filters are nowadays well understood and easy to design and implement. In particular in [10] and [12], specific FIR differentiators have been analysed and designed to reduce the quantization noise. The following formula (taken from [12]) will be used to obtain optimum filter coefficient of an $N-1$ order FIR:

$$b_n = \frac{6}{N(N+1)}\left(1 - \frac{2n}{N-1}\right) = \frac{6(N-1-2n)}{N(N^2-1)} \qquad 0 \le n < N \tag{1.15}$$

Digital IIR differentiators filter are more difficult to design and, even in these days, a lot of efforts have been spent on developing such filters in order to achieve better and better results (see [15], [16] and [17]). However, differently by the FIR, specific IIR differentiator filters that attenuate quantization noise have not been analysed yet and, as already mentioned, is one of the main aims of the project. Since the quantization noise has not a specific band, but it is spread almost all over the frequencies, the filter that will be proposed found a concrete application only in this filed.

The filter design adopted in the remainder of the project is “Model Reduction Approach” (see [16]) and it consists of two stages: first an FIR that satisfies the specification has to be designed and then it will be optimized with previous signal sample in order to obtain an IIR filter.

1.2.3 Phase and group delay

Digital filters, due to their structural complexity, introduce delays in the signal processing, which are bound to the order of the filter and the position of poles.

Given an input signal $x(n)$, with Fourier transform $X(e^{j\omega}) = |X(e^{j\omega})|e^{j\arg(X(e^{j\omega}))}$ (where $|X(e^{j\omega})|$ is the magnitude and $\arg\left(X(e^{j\omega})\right)$ is the phase), and a filter $h(n)$, with Fourier transform $H(e^{j\omega})$, the output signal will be $y(n) = x(n) * h(n)$ or in the frequency domain $Y(e^{j\omega}) = X(e^{j\omega})H(e^{j\omega})$. According to [25], the time delay, known as phase delay, introduced by the filter at the output frequency component $\omega = \omega_0$ is given by:

$$\tau_p(\omega_0) = -\frac{\theta(\omega_0)}{\omega_0}$$

Where $\theta(\omega_0) = \arg\{H(e^{j\omega_0})\}$ is the phase response of the filter at the frequency ω_0.

As measure of linearity of the phase delay will be briefly introduced the group delay:

$$\tau_g(\omega_0) = -\frac{d}{d\omega_0}\theta_u(\omega_0)$$

Where $\theta_u(\omega_0)$ is the unwrapped phase response of the filter.

These delays alter the phase of the various frequencies component of the output signal in different ways and, therefore, it could be necessary to insert an equalizer in cascaded. Altering the signal with a filter that has not a constant group delay could complicate the analysis and design of automatic control system because the signals in the feedback loop should have a constant group delay.

A general FIR filter of order M introduces, during the process, up to M – 1 delay elements. The project involves FIR differentiator which, due to their symmetrical layout, halves the delay, simplifies the filter structure and, the most important, have linear phase (that mean constant group delay). On the other hand, IIR filters of order N, which will be analysed in the remainder of the work, will have N delays element, more complex filter structure and a group delay that is affected by the presence of poles outside the origin (so is not constant).

IIR filters built on FIR inherit the linear phase, nevertheless, in the frequencies that match the phase angle of the poles, the group delay could significantly increase proportionally with the absolute value of the poles. Most of the time, and as we can see in the next chapters, the poles layout will be a trade-off between good noise attenuation and a linear phase (or constant group delay).

1.3 Almost periodic signals and Bohr spectrum

Almost periodic signals (see [26]) have played a significant role in the development of the project and they are a subclass of the almost periodic functions.

As stated in [1] "suppose that $g(t)$ is a continuous, real or complex valued function, defined on $-\infty < t < \infty$, and consider some $\varepsilon > 0$. Any number τ_ε such that

$$|g(t + \tau_\varepsilon) - g(t)| \leq \varepsilon$$

Is called a translation number of $g(t)$ belonging to ε. If in addition, $g(t)$ is such that for every $\varepsilon > 0$ there exists a real number L_ε such that no interval $(t_0, t_0 + L_\varepsilon)$ is free of translation number belonging to ε, $g(t)$ is said to be almost periodic".

The relation between almost periodic signals and the project will be extensively presented in the next chapters but it can be briefly introduced now for the sake of the clarity: when a ramp is quantized and then filtered by a differentiator its error is an almost periodic signal distributed in $[0,1)$ ([12]).

A fundamental property of almost periodic signals is that they are characterised by discrete spectra (see [1]). Unfortunately, due to some numerical limitation on the Signal Processing Toolbox of Matlab (especially in the Discrete Fourier Transform (DFT), where the uniformly spaced frequencies do not necessarily match the discrete spectrum), this property is not always clearly visible at first sight during tests and counterchecks of the theoretical results because the energy of each discrete frequency is spread in the nearby.

A solution of this problem, as proposed in Section 2.5 of [1], can be achieved via two different ways: first, since it will be known at which frequencies the spectrum is not null, will be considered only the first more influent spectral component, and then integrate the DFT raw spectrum in the rounding of the frequencies taken in account. This approximation shows very good results without changing the layout of the plot. Another way is to integrate the spectrum and provide the result on a plot. In this case the spectral power analysed have

to be the raw one because using the spectrum obtained by the first approximation could led to poor results (in fact it would be an approximation of an approximation).

1.4 Digital tachometry

"Digital tachometry involves the derivation of accurate digital estimates to represent the linear or angular velocity of a dynamic system, using information from a digital position sensor, such as an optical incremental encoder" ([1]).

The project is based on the analysis and design of IIR differentiator filters for quantized signals. As it will turn out soon, one of its direct applications is in digital tachometry and velocity estimation: the optical incremental encoder provides quantization signals and the IIR filter estimates the system velocity.

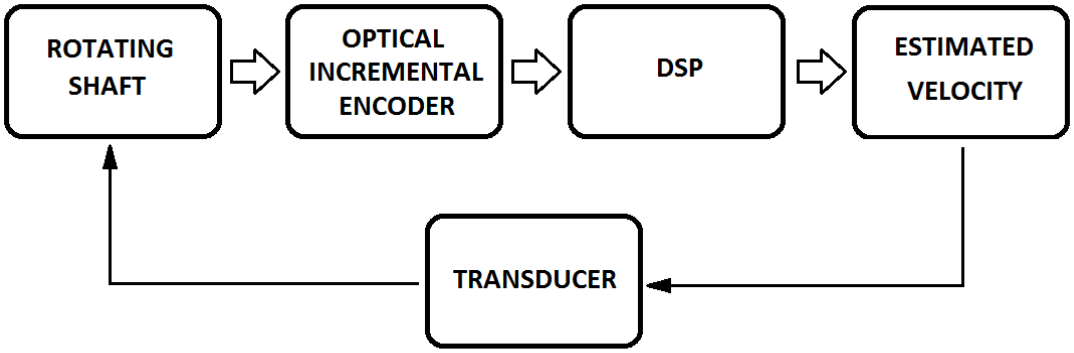

Figure 1.9: Scheme of a possible implementation of a digital tachometer (the feedback arc with the transducer is optional and it is used in control techniques).

Previous works and the state of the art on digital tachometer can be found in [1], [12], [18], [19], [21] and [22]. All these documents regard various aspects of the field of study, however, they never use IIR digital filters: this is the main reason why the project represents a breakthrough and brings a great innovation in the signal processing theory.

In order to simplify the analysis of the various filters, (1.11) has been slightly changed in a form that separates the previous sample by the previous input as given in the following equation:

$$\sum_{k=0}^{N} a_k y(n-k) = s(n) \quad where \quad s(n) = \sum_{k=0}^{M} b_k x(n-k) \tag{1.16}$$

With this little expedient, the theory developed so far on FIR filters can be heavily exploited in the current thesis, considering an FIR filter the one on the right side of (1.16) (it is formed by the b_k coefficients), saving a lot of time and efforts. In addition a coefficient a, named feedback coefficient and domain $[0,1) \in \mathbb{R}$, has been inserted in (1.16) in order to differently weight the previous samples and the input signal. The layout of the formula has been slightly changed to better show the scope of a (in this case the coefficients a_k have opposite sign respect to (1.16)):

$$y(n) = a\sum_{k=1}^{N} a_k y(n-k) + (1-a)s(n) \quad where \quad s(n) = \sum_{k=0}^{M} b_k x(n-k) \tag{1.17}$$

The feedback coefficient can be seen as trade-off between responsiveness of the system and accuracy in output: a small a privileges a quick reaction of the filter, giving more importance to the input. On the other hand, increasing a, the main disadvantage is that the filter reacts slower at quick changes of the input. However, it provides a better approximation of the velocity through previous velocity samples, especially in the constant rate case.

Most of the achievements that will be presented in the following chapter can be applied to every system that involves quantized input signals, as for example Sigma-Delta modulator ([24]). However, particular attentions and specific results will be given and provided in order to analyse the velocity estimation of a constant velocity or slow varying velocity systems.

1.4.1 Constant rate case

The results that will be shown in the remainder of the thesis and based only on filters coefficients will have a general application while, if the results are achieved considering the input signal provided by the optical incremental encoder they are more specific: in the latter case the input signals have constant rate of change (that means constant velocity of the rotating shaft) or their speeds vary very slowly. Figure 1.10 is an example of input signals with different rate and all that signals are provided by an optical incremental encoder as in Figure 1.9.

In the remainder of the work will be used the symbol s to indicate the speed of the rotating shaft or, in the same way, the rate of change of the input signal before quantization. Most of the achievements are function of it or its fractional part $\langle s \rangle$.

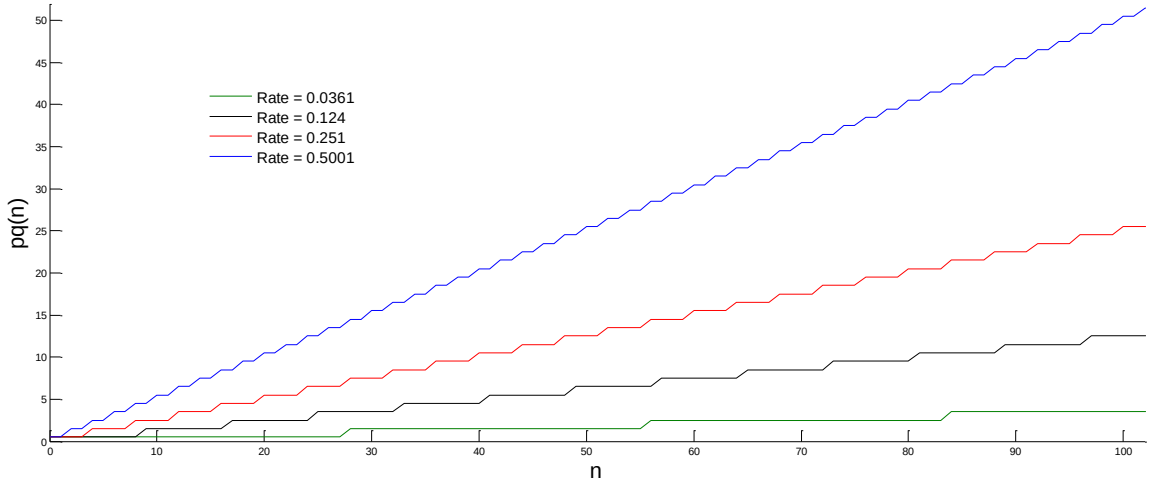

Figure 1.10: Stream of quantized position information as an output of the incremental encoder when the rotating shaft has a constant rate speed.

Given the position information signal:

$$p(n) = p_0 + ns$$

Where n is the sample time, p_0 is the initial position and s is the velocity of the system, the incremental encoder provides the quantized version of it, which is given by:

$$p_q(n) = q\big(p(n)\big) = p(n) + e_p(n) \tag{1.18}$$

Where $e_p(n)$ is the quantization error in the position estimation process.

As stated in [12], when s is irrational (this is not a strict request since every rational number is infinitesimally close to an irrational one), the quantization error $e_p(n)$ is a quasi-stationary process, which provide an almost periodic sequence in the particular case when the input has a constant rate. Then the autocorrelation of $e_p(n)$ is given by (see [1], [12]):

$$R_{e_p}(r) = \sum_{k\neq 0} \frac{1}{4\pi^2 k^2} e^{2\pi jkrs} = \frac{1}{12} - \frac{1}{2}\langle rs\rangle(1 - \langle rs\rangle) \quad r = 0, 1, 2, \dots \tag{1.19}$$

The equation (1.19) is fundamental and it describes the quantization error without approximation and when the only supposition made is the constant rate of change of the input signal. An interesting feature of the formula, which involves s, is that it has the same results with $s = w, w \in \mathbb{R}$ and with $s = w + i, w \in \mathbb{R}$ and $i \in \mathbb{Z}$: two different velocity of the system with the same fractional part have the same correlation for the position error. The property that have been just presented is the main reason why in the resulting plots the

x-axis is labelled with $\langle s \rangle$. The next paragraph will use this formula when an FIR differentiator is considered.

Substituting $x(n)$ with $p(n)$ in (1.16) and considering only its FIR part, will be obtained an FIR digital differentiator:

$$s(n) = \sum_{k=0}^{M} b_k p(n-k) \tag{1.20}$$

The error signal $e_s(n)$ associated to (1.19) is given by:

$$e_s(n) = \sum_{k=0}^{M} b_k e_p(n-k) \tag{1.21}$$

The autocorrelation of the error $e_s(n)$ at the output of the FIR part of the whole filter is given by:

$$\begin{aligned} R_{e_s}(r) &= E[e_s(n)e_s(n-r)] \\ &= E\left[\left(\sum_{\mathrm{k}=0}^{\mathrm{M}} \mathrm{b_k} e_p(\mathrm{n}-\mathrm{k})\right)\left(\sum_{\mathrm{k}=0}^{\mathrm{M}} \mathrm{b_k} e_p(\mathrm{n}-\mathrm{k}-\mathrm{r})\right)\right] \end{aligned} \tag{1.22}$$

Considering that $e_p(n)$ is an almost periodic and almost stationary process (see theory in Section 1.2.1 and Section 1.3) and using its autocorrelation (1.18), the autocorrelation of $e_s(n)$ can be simplified as follow:

$$R_{e_s}(r) = \sum_{h=0}^{M}\sum_{k=0}^{M} \mathrm{b_h b_k R}_{e_p}(\mathrm{r}-\mathrm{h}+\mathrm{k}) \tag{1.23}$$

$$= -\frac{1}{2}\sum_{h=0}^{M}\sum_{k=0}^{M} \mathrm{b_h b_k}\langle(\mathrm{r}-\mathrm{h}+\mathrm{k})\mathrm{s}\rangle(1-\langle(\mathrm{r}-\mathrm{h}+\mathrm{k})\mathrm{s}\rangle) \tag{1.24}$$

All the results that have just been presented are contained in [12]. However, some adaptations have been made to them in order to simplify the comprehension of the work and to exploit them easier in the remainder of the thesis.

From the result above, can be seen that equation (1.23) has a wide range of application inasmuch it depends only in the autocorrelation of the input signal. In spite of it, the achievements will be presented using the more specific (1.24) in order to better understand

the meaning of the formulae and the associated plots. However, since the two equations represent the same quantity, substituting the first in the results that will be presented can leads to a closed solution for every kind of IIR filter and not only for differentiator filters. This is one of the characteristics that bring to the work not only the appeal of being a disruptive innovation in digital tachometry, but also the importance of being a new and general instrument in the DSP analysis field.

Another important aspect of the project is the spectral analysis: while the power spectral density $S(f)$ is commonly used in order to analyse general signals, with quantized signals it is better to consider the power spectrum $P(f)$. This distinction is necessary when is used the Bohr spectrum to estimate the frequency domain behaviour of the error process because it could lead to numerical problems.

Due to the assumptions of unity sample time and the unity bins of the incremental optical encoder the power spectrum of the input is periodic with period one. Moreover, since the used filters have real coefficients the frequency response, phase and group delay has even symmetry. This is the reason why most of the plot will have in the x-axis [0, 0.5] as domain and the frequencies will be labelled with $\langle s \rangle$.

According to these preliminary remarks on the spectrum analysis and the result achieved in [1] on the power spectrum of e_p(n) is given by:

$$P_{e_p}(f) = \begin{cases} \dfrac{1}{4\pi^2 k^2} & k \neq 0 \\ 0 & k = 0 \end{cases} \qquad \forall f = \langle ks \rangle \tag{1.25}$$

Equation (1.25) shows that the power spectrum of the input error, when the velocity of the rotating shaft is constant, is discrete and nonlinearly dependent on $\langle s \rangle$. Moreover, the spike of $P_{e_p}(f)$ are not equally distributed as in the Sigma-Delta modulation (see [23]), but they are spaced by $\langle s \rangle$.

The power spectrum expected at the output of the IIR digital differentiator is the same given by (1.25) rescaled by the magnitude response of the filter. In other words, since the filter has not properties as upsamplig or downsampling, the power spectrum at the output has the spikes in the same frequencies denoted by (1.25), but rescaled with the particular magnitude response of the filter in that particular frequencies.

An example application of (1.25) is given by Figure 1.11, where a power spectrum of a simulation with $\langle s \rangle = 0.1143$ is depicted.

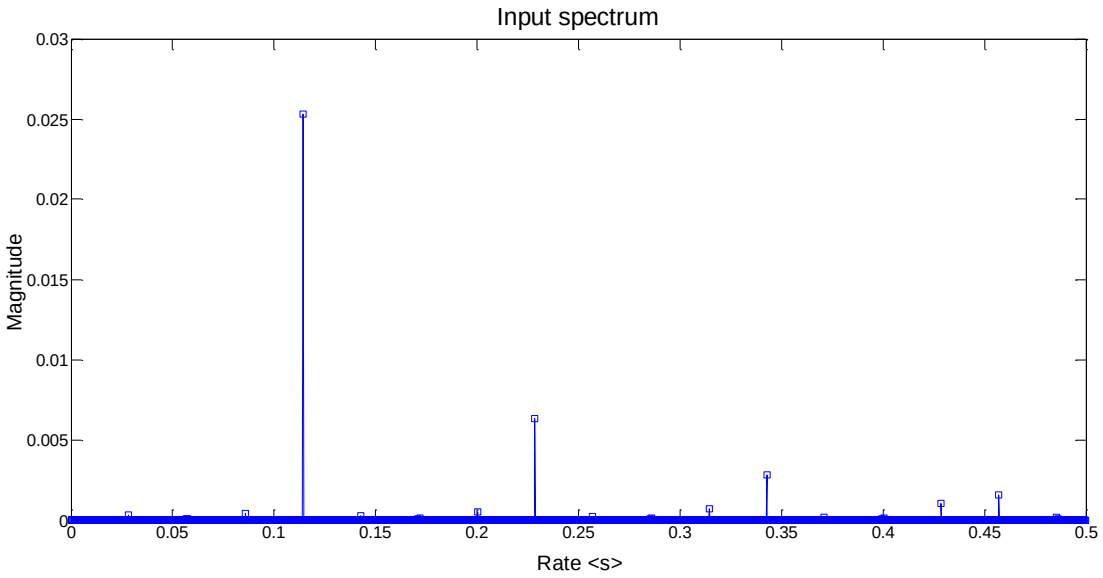

Figure 1.11: Power spectrum of an input signal given by a quantized ramp with slope $\langle s \rangle = 0.1143$.

In the particular case of Figure 1.11 seems that a low pass filter could be the best choice. However, since the fractional part of the rate of change is not known a priori, the optimization of the IIR differentiator cannot be done as low pass filter: with $\langle s \rangle$ close to 0.5 a high pass filter would achieve better results. In general, a filter will be considered optimum if it evenly attenuates the MSE at the output, without considering the effects on the power spectrum, so there are no distinctions between high and low rates.

2 First order IIR digital differentiator

The first order IIR digital differentiator is the simplest case of IIR differentiator. As it will turn out in the next sections, this kind of filter has some advantages in the analysis and even more in the design if compared with higher order filters of the same type. Both numerator and denominator of the transfer function of the differentiator are polynomials of order $N = M = 1$ in the variable z^{-1}.

2.1 The filter

The numerator, as seen in section 1.2.2, has optimal coefficient derived by (1.15) and they are $b_0 = 1$ and $b_1 = -1$. Basically, it is the first order FIR digital differentiator and, according to (1.16), it is given by:

$$s(n) = b_0 p(n) + b_1 p(n-1) = p(n) - p(n-1) \tag{2.1}$$

Where $p(n)$ is the output of the incremental optical encoder that provides position information at the sample time n.

The autocorrelation of the signal $e_s(n)$, which is the error associated at the signal $s(n)$ and it is obtained by (1.21), is given by (using (1.19), (1.23) and (1.24) with $M = 1$):

$$R_{e_s}(r) = 2\mathrm{R}_{e_p}(\mathrm{r}) - \mathrm{R}_{e_p}(\mathrm{r}-1) - \mathrm{R}_{e_p}(\mathrm{r}+1) \tag{2.2}$$

$$= \frac{1}{2}[\langle(\mathrm{r}-1)\mathrm{s}\rangle(1 - \langle(\mathrm{r}-1)\mathrm{s}\rangle) + \langle(\mathrm{r}+1)\mathrm{s}\rangle(1 - \langle(\mathrm{r}+1)\mathrm{s}\rangle) - 2\langle\mathrm{rs}\rangle(1 - \langle\mathrm{rs}\rangle)] \tag{2.3}$$

In order to obtain the first order IIR digital differentiator, the previous velocity sample has to be added to (2.1), as shown in (1.17). The final result is given by:

$$v(n) = av(n-1) + (1-a)s(n) = av(n-1) + (1-a)[p(n) - p(n-1)] \quad (2.4)$$

The transfer function derived by (2.4) is given by:

$$H(z) = (1-a)\frac{1-z^{-1}}{1-az^{-1}} \quad (2.5)$$

As said above this is the simplest differentiator with an infinite impulse response and it can be confirmed by noticing that in (2.4) and (2.5) the only parameter that can vary during the analysis or the design of this filter is the feedback coefficient a. However, the intrinsic simplicity of the filter has given some trouble in the examination of higher order because the lack of generality hides some fundamental aspects necessary to achieve good results. This property will be presented in the next chapters.

2.1.1 Zero-Pole layout

Analyzing (2.5), it is easy to deduce that the zero is in $(1,0) \in \mathbb{C}$ and the pole is in $(a,0) \in \mathbb{C}$. Since the filter has real coefficient and the domain for the feedback coefficient is $[0,1)$ the only pole can move on the real axis from $(0,0) \in \mathbb{C}$ to a point infinitesimally closed to $(1,0) \in \mathbb{C}$.

As will be shown more in detail in Section 2.1.2 the position of the pole, which in this particular case is determined by a, is the responsible for the trade-off between attenuation of the noise and preserving a linear phase (so a constant group delay). Both factors are very important in filter design and unfortunately they cannot be achieved in an optimum way at the same time.

Figure 2.1 shows the zero pole layout in the complex plane with the unity circle (obtained with the zplane(num, den) function of Matlab): the zero is the little circle in $(1,0) \in \mathbb{C}$ while are depicted various solution for the pole in $(a,0) \in \mathbb{C}$ for different values of a in its domain.

One property hidden in the filter structure, which was erroneously taken for granted during the development of the project, is that the pole has always the same phase angle of the zero, whatever would be the value of a. In the next chapters, with IIR digital differentiators of higher orders, will be shown that the feature just presented plays a fundamental role to achieve a good attenuation of the quantization noise.

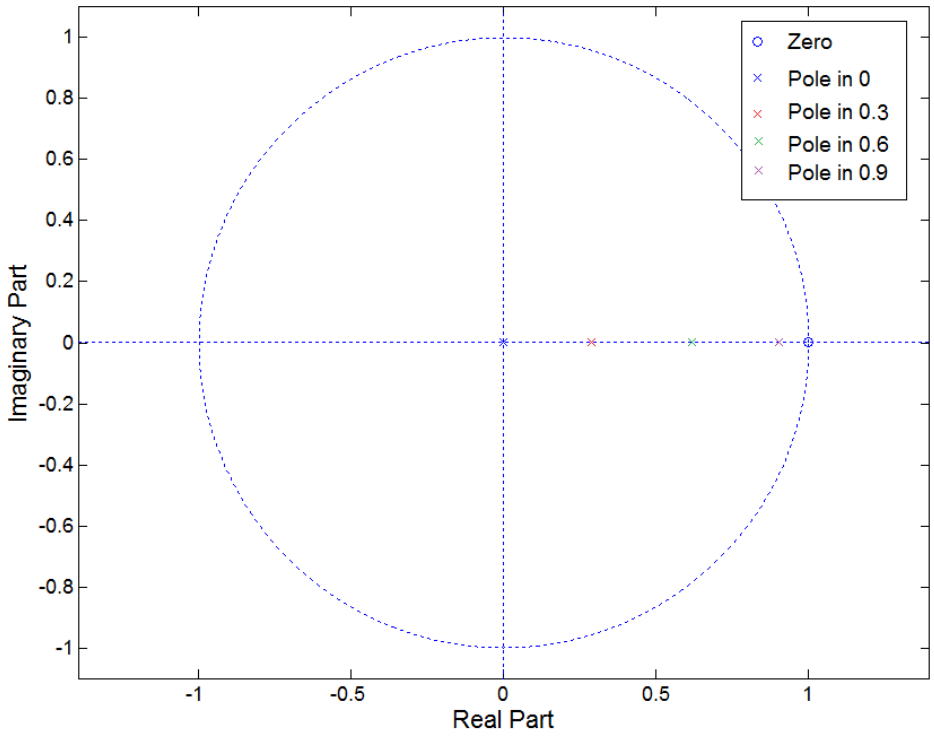

Figure 2.1: Zero-Pole layout for a first order IIR digital differentiator. Here are depicted the poles for four different values of the feddback coefficient a.

2.1.2 Magnitude, phase and group delay of the differentiator

The feedback coefficient a can change the overall behavior of the IIR digital differentiator in terms of frequency response: the following plots show how the magnitude, the phase and

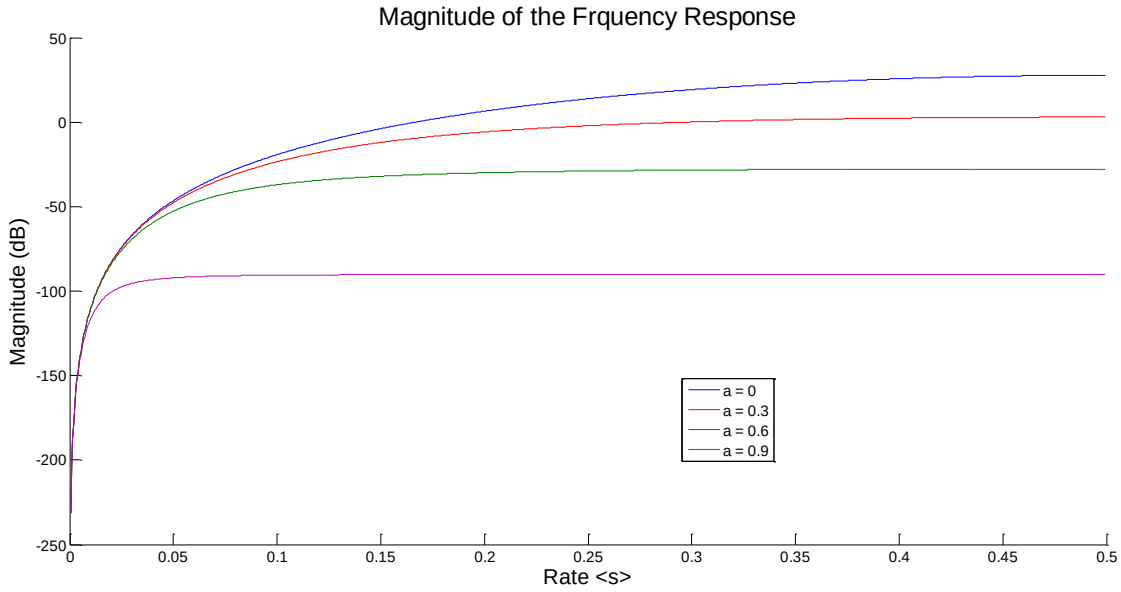

Figure 2.2: Frequency response (on the normalized frequencies $[0, 1)$) of the first order IIR digitla differentiator for variuos value of the feedback coefficient.

the group delay of the filter change as higher as a become. In the figures is depicted only half rate $\langle s \rangle$ domain in order to better appreciate the shape of the function; it has been possible due to the symmetry of the plots.

As depicted in Figure 2.2 the differentiator achieve better and better noise attenuation when a increase. On the other hand Figure 2.3 and Figure 2.4 show that the filter introduces high phase distortion and non-constant group delay in the signal when a assumes high values.

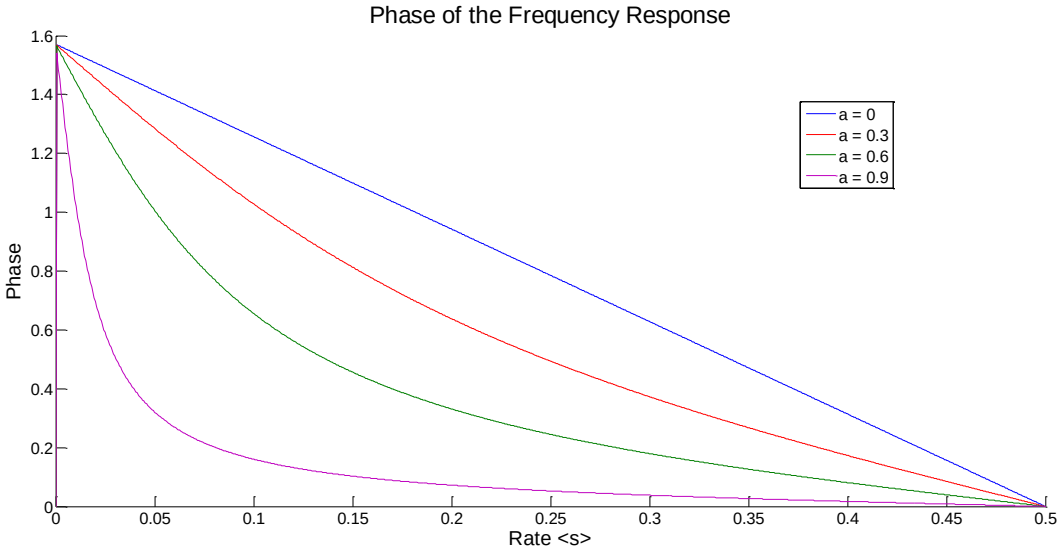

Figure 2.3: Phase of the first order IIR digital differentiator for different value of the feedback coefficient.

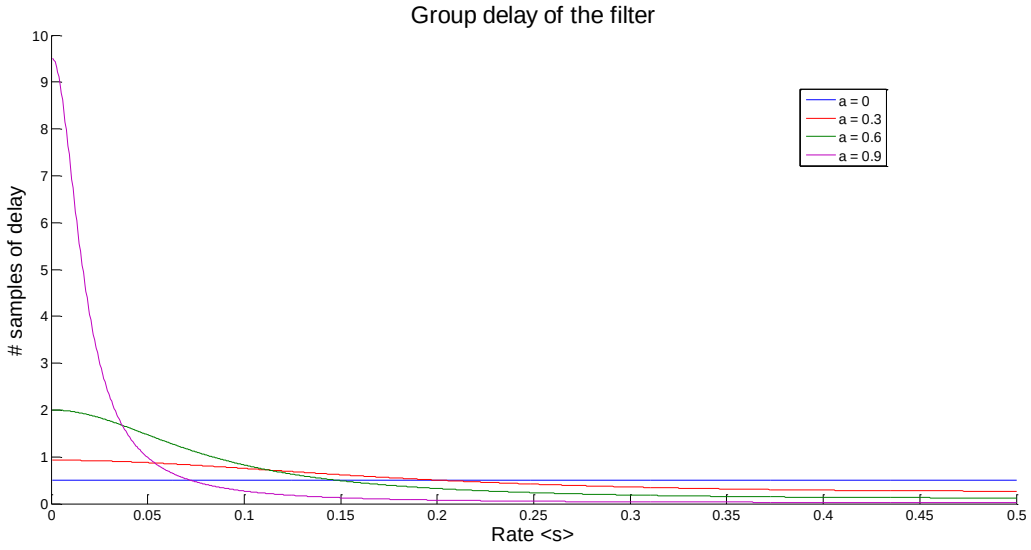

Figure 2.4: Group delay of the first order IIR digital differentiator for different value of the feedback coefficient.

Comparing Figure 2.2 and Figure 2.4 is easy to understand why a is the trade-off between noise attenuation and responsiveness of the filter: with $a = 0$ the filter behave as a simple FIR differentiator with a linear phase and a constant group delay. On the other hand with $a = 0.9$ a complete noise deletion can be almost reached. However, in the latter case the group delay makes the output of the filter useless in a close loop control without an appropriate equalizer.

2.2 Quantization mean square error

The first approach in order to achieve the quantization mean square error formula of the first order IIR digital differentiator was made in the time domain: looking at the plot of the error at the output of the filter, some connection with the Farey Sequence[1] came up, but the entire analysis would be too complicated. However, all the plots of the outcomes of the filter and the error associated at the estimation of the velocity in the time domain have simplified the work done, because they were useful to understand what would be the correct expectation from the results of the project and to check and eventually adjust possible mistakes in the formulae.

The second approach was in the frequency domain: since the quantization error has discrete spectrum, some similarities with [23] was found. Although a lot of the literature on Sigma-Delta modulation had been taken in account, no other connections, help or simplifications were found in that field. Nevertheless, some of the achievements of this thesis could be easily applied to analyse the behaviour of Sigma-Delta modulator.

The successful approach in order to obtain the MSE at the output of the IIR differentiator was based on section 1.2.1 and more in general in that described in the second chapter of [24]: using autocorrelation and cross-correlation, a system of equations has been derived and after finding it solution, from one of the variables it was possible to infer the $R_{e_v}(0)$, which corresponds to the MSE at the output of the IIR differentiator.

Starting from equation (2.4), will be considered its associated error formula in order to calculate $R_{e_v}(0)$. It is given by:

$$e_v(n) = ae_v(n-1) + (1-a)e_s(n) \tag{2.6}$$

[1] See http://en.wikipedia.org/wiki/Farey_sequence

Now, multiplying both sides of (2.6) by its terms, so $e_v(n)$, $e_v(n-1)$ and $e_s(n)$, a system formed by three equations is obtained in (2.7).

$$\begin{aligned} e_v(n)e_v(n) &= ae_v(n-1)e_v(n) + (1-a)e_s(n)e_v(n) \\ e_v(n)e_v(n-1) &= ae_v(n-1)e_v(n-1) + (1-a)e_s(n)e_v(n-1) \\ e_v(n)e_s(n) &= ae_v(n-1)e_s(n) + (1-a)e_s(n)e_s(n) \end{aligned} \quad \textbf{(2.7)}$$

Both $e_v(n)$ and $e_s(n)$ are error signal that are almost stationary and quasiperiodic so, using the theory in sections 1.2.2 and 1.3, it is possible to take the expectation of (2.7) and obtain what follow by (1.8) and (1.9).

$$\begin{aligned} \mathrm{R_{e_v}}(0) &= \mathrm{aR_{e_v}}(1) + (1-\mathrm{a})\mathrm{R_{e_{vs}}}(0) \\ \mathrm{R_{e_v}}(1) &= \mathrm{aR_{e_v}}(0) + (1-\mathrm{a})\mathrm{R_{e_{vs}}}(-1) \\ \mathrm{R_{e_{vs}}}(0) &= \mathrm{aR_{e_{vs}}}(-1) + (1-\mathrm{a})\mathrm{R_{e_s}}(0) \end{aligned} \quad \textbf{(2.8)}$$

The new system has $R_{e_v}(0)$, $R_{e_v}(1)$, $R_{e_{vs}}(0)$ and $R_{e_{vs}}(-1)$ as variable so, in order to make the system solvable with an unique solution , another equation (independent form the given) is needed. Should be noticed that $R_{e_s}(0)$ is not a variable because its value can be easily derived using (2.2) or (2.3).

Substituting the $e_v(n-1)$ term in right side of (2.6) with the next equation

$$e_v(n-1) = ae_v(n-2) + (1-a)e_s(n-1) \quad \textbf{(2.9)}$$

And performing this process in a recursively way[2], the resulting equation is given by:

$$e_v(n) = (1-a)\sum_{k=0}^{\infty} a^k e_s(n-k) \quad \textbf{(2.10)}$$

Now, simply multiplying both sides of (2.10) by $e_s(n)$ and taking its expectation, the cross-correlation between $e_v(n)$ and $e_s(n)$ in the origin is obtained. Adding it to (2.8), a new system of four equations and four variables is obtained and it is given by (2.11)

[2] See http://mathworld.wolfram.com/LinearRecurrenceEquation.html

$$R_{e_v}(0) = aR_{e_v}(1) + (1-a)R_{e_{vs}}(0)$$

$$R_{e_v}(1) = aR_{e_v}(0) + (1-a)R_{e_{vs}}(-1)$$

$$R_{e_{vs}}(0) = aR_{e_{vs}}(-1) + (1-a)R_{e_s}(0) \quad \textbf{(2.11)}$$

$$R_{e_{vs}}(0) = (1-a)\sum_{k=0}^{\infty} a^k R_{e_s}(k)$$

The purpose of the project does not need the entire solution of the system but only $R_{e_v}(0)$, which corresponds to the quantization MSE. So, the resolution of the system will be made only to achieve that result.

The next step consists in deriving $R_{e_{vs}}(-1)$ from the third equation and make it depends only on the autocorrelation of $e_s(n)$. It can be done substituting $R_{e_{vs}}(0)$ with the value hold by the fourth equation. The result is shown in (2.12).

$$R_{e_{vs}}(-1) = \frac{R_{e_{vs}}(0) - (1-a)R_{e_s}(0)}{a} = \frac{(1-a)\sum_{k=0}^{\infty} a^k R_{e_s}(k) - (1-a)R_{e_s}(0)}{a} \quad \textbf{(2.12)}$$

The last step provides the final result: solving the system formed by the first two equations of (2.11) in the variables $R_{e_v}(0)$ and $R_{e_v}(1)$, then substituting in the result for $R_{e_v}(0)$ the equations for $R_{e_{vs}}(0)$ and $R_{e_{vs}}(-1)$ (fourth of (2.11) and (2.12) respectively), is possible to derive the following formula for $R_{e_v}(0)$:

$$MSE_{e_v} = R_{e_v}(0) = 2\frac{1-a}{1+a}\left[\sum_{k=0}^{\infty} a^k R_{e_s}(k) - \frac{R_{e_s}(0)}{2}\right] \quad \textbf{(2.13)}$$

The closed form solution (2.13) can be seen as the MSE at the output of the filter given by the following equation

$$H(z) = \frac{1-a}{1-az^{-1}}$$

when in input there is the signal $e_s(n)$. However, the main aim of the project is to infer a formula for the "real" input that is $e_p(n)$. Substituting (2.2) in (2.13) the formula for MSE_{e_v} can be derived and it is given by:

$$MSE_{e_v} = 2\frac{1-a}{1+a}\left[\sum_{k=0}^{\infty} a^k \left(2\mathrm{R}_{e_p}(\mathrm{k}) - \mathrm{R}_{e_p}(\mathrm{k}-1) - \mathrm{R}_{e_p}(\mathrm{k}+1)\right) - \mathrm{R}_{e_p}(0) + \mathrm{R}_{e_p}(1)\right] \quad \textbf{(2.14)}$$

This is a very general result and can be applied in every DSP project that involves IIR digital differentiators of the first order. Moreover, with little adjustments in the calculation of $R_{e_s}(r)$ this result can be also extender to IIR filter that are not strictly differentiator, giving at the formula the more universal meaning possible. The only request to calculate MSE_{e_v} is to have previously inferred $\mathrm{R}_{e_p}(\mathrm{r})$, but usually this is not a problem because the input error is usually well understood and analysed.

Substituting (2.3) in (2.13), the particular case of a quantized ramp provided by an incremental optical encoder in a digital tachometer can be obtained as closed form solution in (2.15). This result represents the real innovation in the field of digital tachometry because IIR differentiators have never been analysed in such manner before.

$$MSE_{e_v} = \frac{1-a}{1+a}\left[\sum_{k=0}^{\infty}\left[a^k[\langle(\mathrm{k}-1)\mathrm{s}\rangle(1-\langle(\mathrm{k}-1)\mathrm{s}\rangle)+\langle(\mathrm{k}+1)\mathrm{s}\rangle(1-\langle(\mathrm{k}+1)\mathrm{s}\rangle) - 2\langle\mathrm{ks}\rangle(1-\langle\mathrm{ks}\rangle)]\right]-\langle\mathrm{s}\rangle(1-\langle\mathrm{s}\rangle)\right] \quad \textbf{(2.15)}$$

Can be seen that when $a = 0$ the solution is simply $MSE_{e_v} = \langle\mathrm{s}\rangle(1-\langle\mathrm{s}\rangle)$, which corresponds at the quantization mean square error of the first order FIR digital differentiator (see [1] and [12]).

Equation (2.15) is the closed form solution of the quantization mean square error of the first order IIR digital differentiator. Experimental proofs, on the correctness of the formula which has just been proposed, have been developed in Matlab and they guarantee the rightness of MSE_{e_v}: the average absolute difference, between the theoretical and experimental results, is about 10^{-6}, which can be caused by numerical approximation of the Toolbox of Matlab, the transient phase of the filter and the nonzero initial position.

Figure 2.5 shows the MSE at the output of the filter in function of the fractional part of the input speed s. It can be seen that with $a = 0.9$ the noise is almost cancelled (average value around 10^{-3}). Nevertheless, in this case the group delay at low rates can be very high as depicted in Figure 2.4. The feedback coefficient a has to be carefully chosen in order to satisfy all constrains of the project that has to be developed on noise attenuation and flattening of the group delay, especially when the estimated velocity is used in a close loop control system.

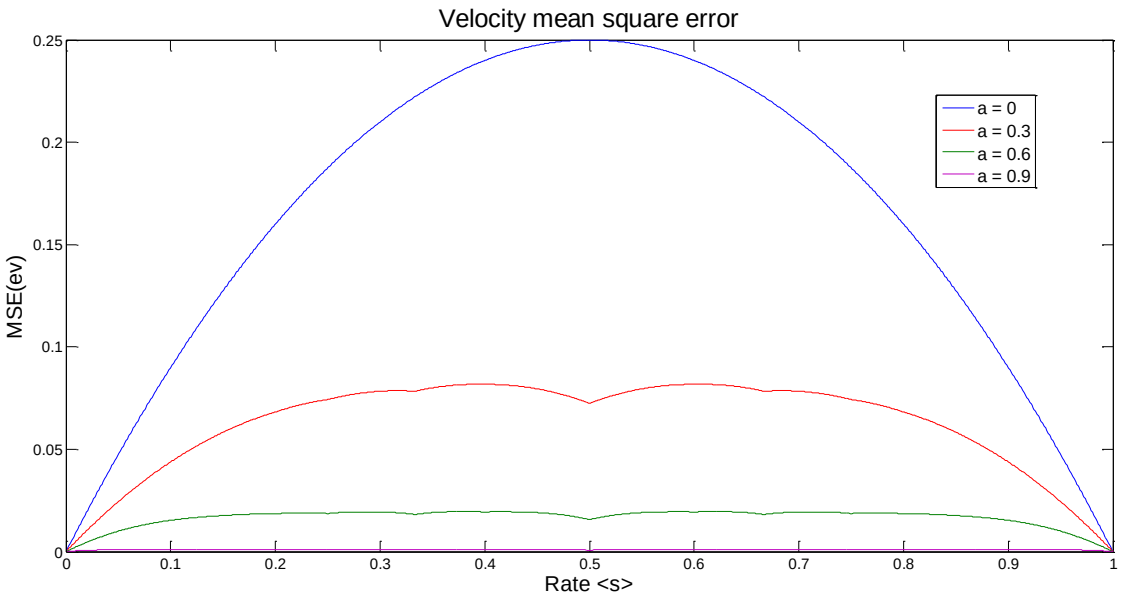

Figure 2.5: Velocity estimation mean square error of the first order IIR digital differentiator for different value of the feedback coefficient.

2.3 Comparison with the white noise assumption

The noise introduced in the system by the quantizer cannot be represented by a linear function so, in order to simplify the analysis, it has been often modelled as white noise on the interval [-0.5, 0.5] (see section 1.1.3).

The Åström, Juri and Agniel algorithm (see section 1.2.1) has been applied to (2.6) in order to derive the white noise approximation of the quantization noise for the first order IIR digital differentiator. The formula obtained by the algorithm does not take in account the correlation of the noise. It is given by:

$$R_w = 2\frac{(1-a)^2}{1+a} \tag{2.16}$$

Now, if the quantization noise is considered white noise on the interval [-0.5, 0.5], it has a variance which is given by $(b-a)/12$ and in this particular case is equal to $1/12$. Rescaling (2.16) with this factor gives the following result:

$$R_{w_v} = \frac{(1-a)^2}{6(1+a)} \tag{2.17}$$

In order to check the correctness of (2.17) with experimental data, the average of MSE_{e_v} has been calculated using Matlab and the (2.18), since the white noise approximation represents the average value of the real mean square error.

$$R_{w_{exp}} = \int_0^1 R_{e_v}(0)\, d\langle s \rangle \tag{2.18}$$

The experimental results tell that (2.17) and (2.18) perfectly match so the validity of (2.17) is proven. In the following plots is shown only one line for both quantities due to their equality.

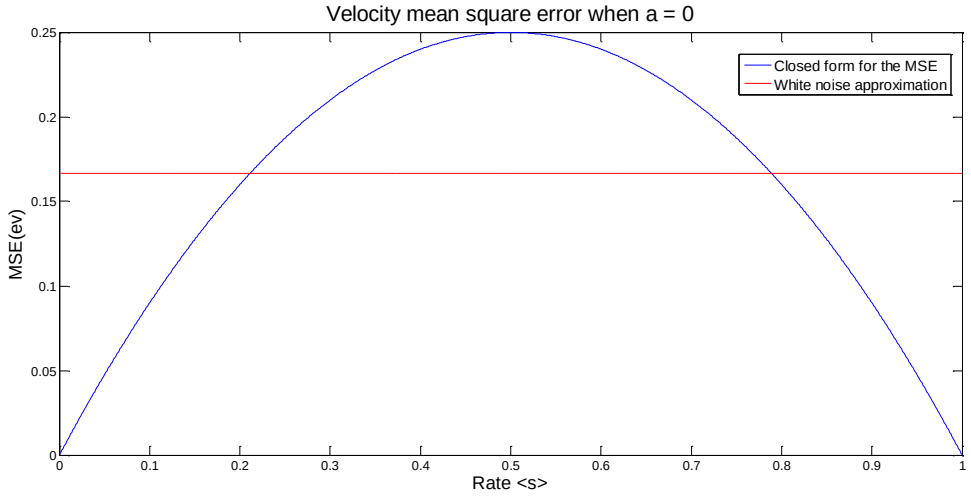

Figure 2.6: Comparison between the output MSE and the white noise approximation when $a = 0$.

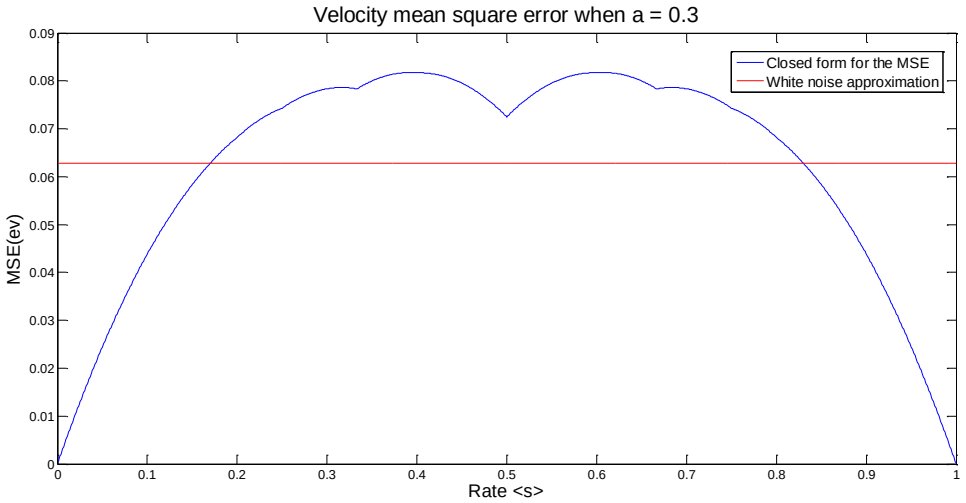

Figure 2.7: Comparison between the output MSE and the white noise approximation when $a = 0.3$.

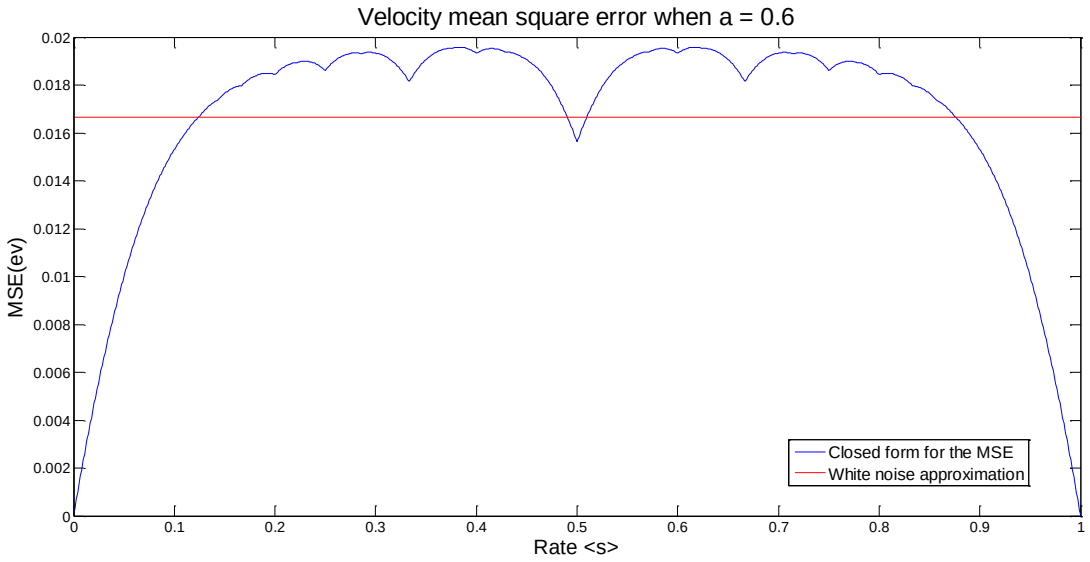

Figure 2.8: Comparison between the output MSE and the white noise approximation when $a = 0.6$.

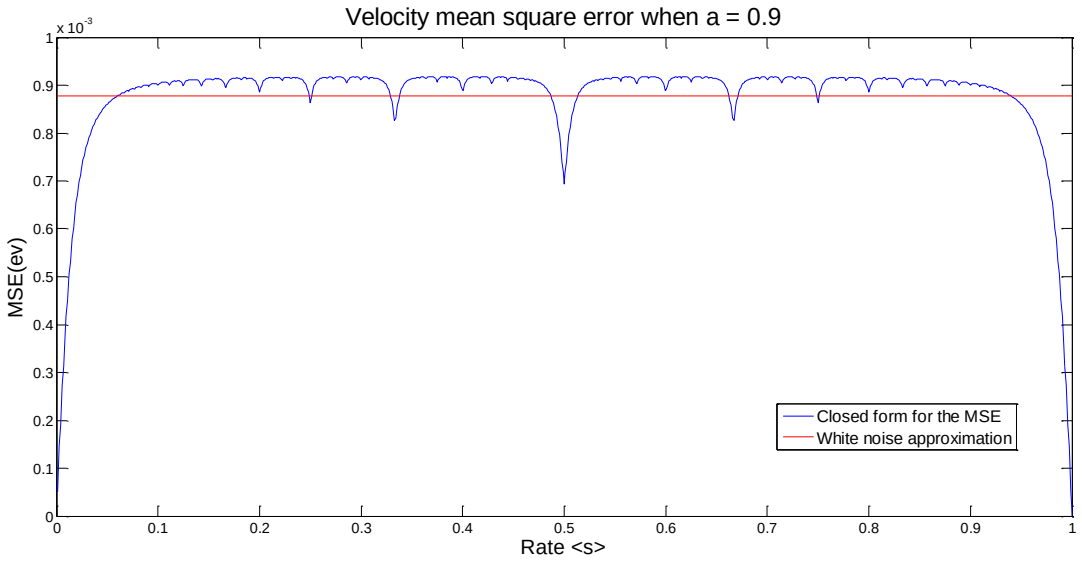

Figure 2.9: Comparison between the output MSE and the white noise approximation when $a = 0.9$.

Figure 2.6 to Figure 2.9 show the comparison between the real shape of the quantization mean square error at the output of the differentiator and the common assumption that models the quantization noise as white noise. In the first three plots is easy to understand why the approximation could lead to poor results: the two shapes are very different and MSE_{e_v} is far from being flatten. In the last plot, instead, the value of the feedback coefficient is high enough to make sure that the two functions are quite close. In this case the white

noise approximation could be used as substitute, but it is better to keep in mind that the real MSE could be worse than the approximation.

Anyway, the white noise approximation provides values that in some rates are smaller than the effective quantization mean square error. If the measurements are used in an open loop system, the property just presented affects only the truthfulness of the results. On the other hand, this fact could introduce unexpected or unstable behaviours in a system, if the measurement is used as feedback in a close loop control function. Due to this motivation the aim to find a worst case approximation was added at the project during its development. It will be presented in the next section.

2.4 Worst case approximation

The worst case approximation, as the white noise approximation, is an estimation of the quantization mean square error at the output of the IIR differentiator. Despite the case presented in the previous section, this one provides a value that corresponds to the worst case of MSE_{e_v} for the various value of the feedback coefficient. With this expedient, the approximation that is going to be proposed can also be used in systems that insert the estimated velocity in a close loop control function, without unwanted behaviour.

At the beginning, the aim of the project was to discover both the value of the worst case and the rate $\langle s \rangle$ at which occurs. Due to the high complexity of the work and the relatively poor interest in the rate the project was focused on the worst case only.

A first, raw, attempt to derive the formula for the approximation has been made using a rescaled version of (2.17): the only constrain was that at least when $a = 0$ the result from the formula matches the real worst case. Under these assumptions, the scaling factor has been researched through equation (2.15), which models the FIR differentiator and whose MSE at the output is given by:

$$MSE_{e_v} = MSE_{e_s} = \langle \mathrm{s} \rangle (1 - \langle \mathrm{s} \rangle) \tag{2.19}$$

Using simple mathematical analysis is easy to find the maximum of (2.19) in $\langle \mathrm{s} \rangle = 0.5$ whose value is 0.25. The final approximation formula is given by:

$$R_{wc_v} = 0.25 \frac{(1-a)^2}{(1+a)} \tag{2.20}$$

The results from (2.20), the real value of the worst case of MSE_{e_v} and the percentage difference between them is summarized in the table below for various values of a:

a	Approximation (2.20)	Real value (2.15)	Percentage difference
0	0.250000000000000	0.250000000000000	0.00
0.1	0.184090909090909	0.171906335799378	6.62
0.2	0.133333333333333	0.119675647994255	10.24
0.3	0.0942307692307692	0.0817463493255846	13.25
0.4	0.0642857142857143	0.0539432579361614	16.09
0.5	0.0416666666666667	0.0337968365708230	18.89
0.6	0.0250000000000000	0.0195818193551980	21.67
0.7	0.0132352941176471	0.00999671241306348	24.47
0.8	0.00555555555555555	0.00403866883246570	27.30
0.9	0.00131578947368421	0.000918102447361396	30.22

Despite it was only a raw attempt and its results are far from be good, the table above shows an interesting pattern in the percentage difference value: except when $a = 0$, the values have an almost linear rate of increment (about 3%) with an offset of 3%. Evaluating this aspect of the outcomes, (2.20) has been split in two cases: $a = 0$ and $a \neq 0$. In the latter a corrective factor, with 3% of offset and rate, has been inserted in the formula in order to achieve a better approximation. The resulting formula is given by:

$$R_{wc_v} = \begin{cases} 0.25 & when\ a = 0\ (FIR) \\ 0.25\,\dfrac{(1 - 0.3(a + 0.1))(1 - a)^2}{1 + a} & when\ a \neq 0 \end{cases} \quad \textbf{(2.21)}$$

The outcomes from the new worst case approximation of MSE_{e_v} are summarized in the table below:

a	Approximation (2.21)	Real value (2.15)	Percentage difference
0	0.250000000000000	0.250000000000000	0.00
0.1	0.173045454545455	0.171906335799378	0.658
0.2	0.121333333333333	0.119675647994255	1.366
0.3	0.0829230769230769	0.0817463493255846	1.419
0.4	0.0546428571428571	0.0539432579361614	1.280
0.5	0.0341666666666667	0.0337968365708230	1.082
0.6	0.0197500000000000	0.0195818193551980	0.852
0.7	0.0100588235294118	0.00999671241306348	0.617
0.8	0.00405555555555555	0.00403866883246570	0.416
0.9	0.000921052631578947	0.000918102447361396	0.320

The average percentage difference is now about 0.8% and has a worst case about 1.4% so the results from (2.21) could be considered reliable and no more investigation are needed in this approximation.

Figure 2.10 shows the comparison between the worst case approximation, which has just been proposed, the white noise approximation and the real mean square error. Can be seen that when the feedback coefficient is high enough (as in Figure 2.10 d), the worst case approximation can almost be considered the same function as the real MSE, giving very good result if used.

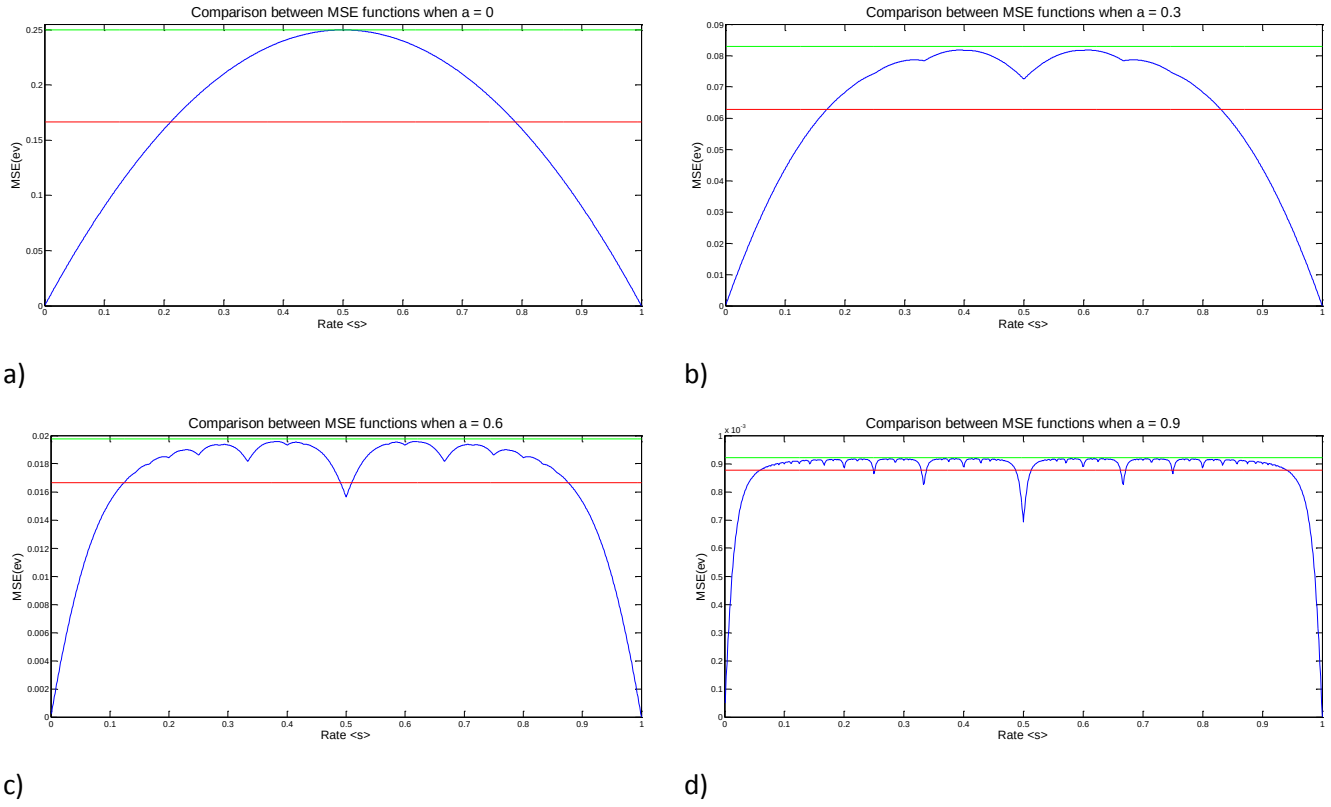

Figure 2.10: Comparison between worst case approximation (green), white noise approximation (red) and real output mean square error (blue) for different values of a: a) $a = 0$, b) $a = 0.3$, c) $a = 0.6$ and d) $a = 0.9$.

2.5 Spectral analysis

The last aim of the project involves the spectral analysis of the first order IIR digital differentiator: considering the power spectrum of the input error, which is given by (1.25), and the transfer function of the filter, which is given by (2.5), the work done and the

experimental results have as a result a close form solution for the power spectrum of the quantization error at the output of the filter.

The frequency response associated to (2.5) is given by:

$$H(e^{jw}) = (1-a)\frac{1-e^{-jw}}{1-ae^{-jw}} \tag{2.22}$$

Now, in order to calculate the power spectrum of the output signal, the square magnitude of (2.22) is needed. It is given by:

$$\left|H(e^{jw})\right|^2 = (1-a)^2\frac{\left|1-e^{-jw}\right|^2}{|1-ae^{-jw}|^2} = (1-a)^2\frac{2(1-\cos(2\pi ks))}{1+a^2-2a\ \cos(2\pi ks)} \tag{2.23}$$

The power spectrum of the output signal is obtained multiplying the power spectrum in input, (1.25), by the square magnitude of the filter, (2.23). The following formula gives the final result:

$$P_{e_v}(f) = \begin{cases} \dfrac{(1-a)^2}{2\pi^2 \mathrm{k}^2}\dfrac{1-\cos(2\pi ks)}{1+a^2-2a\ \cos(2\pi ks)} & k \neq 0 \\ 0 & k = 0 \end{cases} \qquad \forall\, f = \langle ks \rangle \tag{2.24}$$

In order to prove the correctness of (2.24), some Matlab tests have been developed. Using large datasets it has been possible to plot the power spectrum for the theoretical and the experimental results. For the sake of clarity only the first twenty spectral components of (2.24) will be considered ($k \in \{1, \dots, 20\}$) because the magnitude of the spikes decrease in a quadratic fashion. Figure 2.11 is the power spectrum depicted in Figure 1.11 after the filtering process. It shows that the experimental data (blue) and the results obtained from (2.24) (red cross) perfectly matches so, the rightness of the equation (2.24) is eventually proved.

The input error spectrum is provided by (1.25) and the particular case when $s = 0.1143$ is depicted in Figure 1.11. Comparing Figure 1.11 and Figure 2.11 is easy to see that both are discrete and with the same nonzero frequencies. The only difference is in the magnitude of the spectrum, which is rescaled by the magnitude depicted in Figure 2.2.

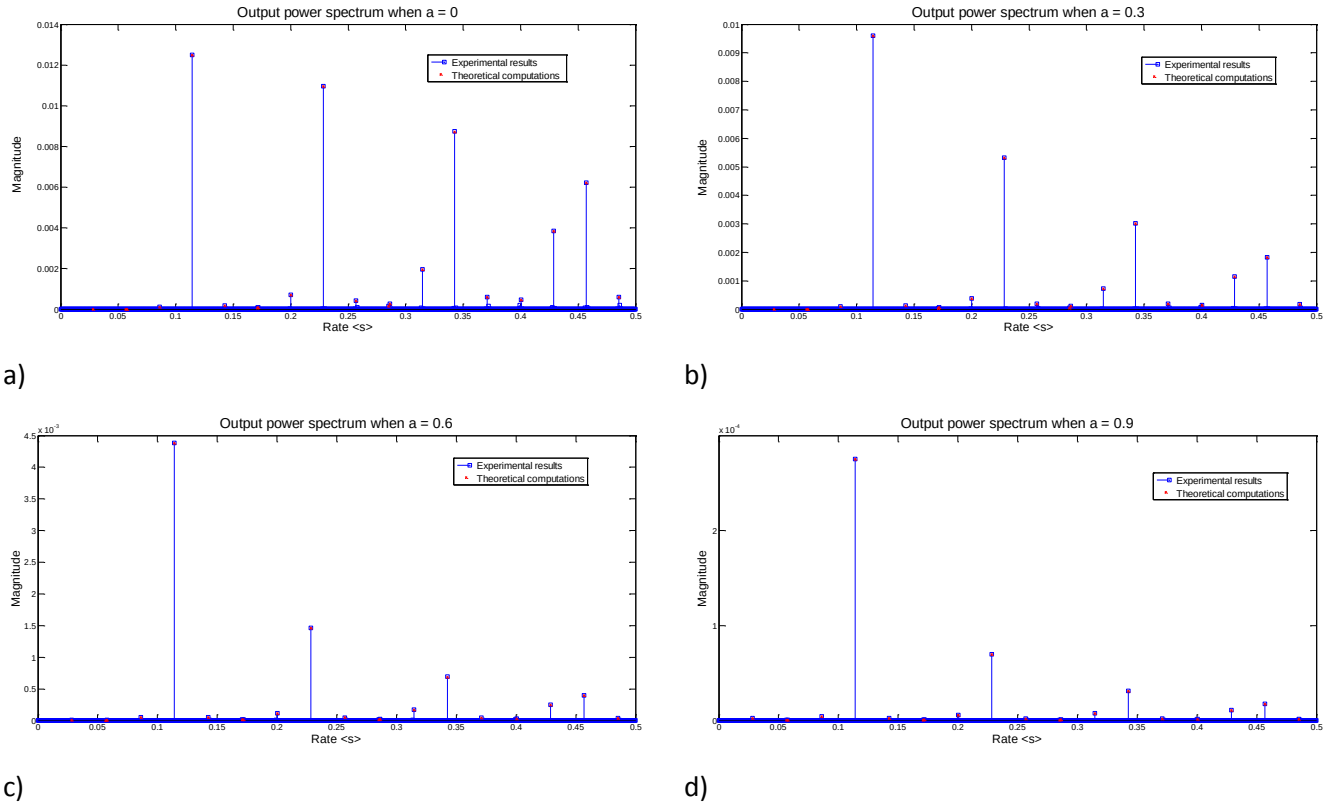

Figure 2.11: Comparison between the theoretical and the experimental results with input rate $s = 0.1143$ and for different values of a: a) $a = 0$, b) $a = 0.3$, c) $a = 0.6$, d) $a = 0.9$

3 Second order IIR digital differentiator

The work done on the second order IIR digital differentiator is similar to the one presented for the first order so, the outline of this chapter is the same of the previous. Nevertheless, some aspects regarding filter coefficient and close form solutions have peculiar differences that are really worth to be discussed because, as previously said, the first order IIR differentiator has some lacks of generality.

Both numerator and denominator of the transfer function of the filter are polynomials of order $N = M = 2$ in the variable z^{-1}.

3.1 The filter

The optimal filter coefficients for the numerator are, again, chosen using (1.15) and they are $b_0 = 1/2$, $b_1 = 0$ and $b_2 = -1/2$. The FIR part of the whole filter is given by:

$$s(n) = \frac{1}{2}[p(n) - p(n-2)] \tag{3.1}$$

The error signal $e_s(n)$ which is related to (3.1) is obtained using (1.21) and it is given by:

$$e_s(n) = \frac{1}{2}[e_p(n) - e_p(n-2)] \tag{3.2}$$

The layout of (3.2) is similar to the error signal associated to (2.1) but this filter achieves better results because it considers positions information that are separated by two time sample so, also the error is rescaled by a factor two. In this case the quantization mean square error of the filter is like the MSE of the first order FIR digital differentiator rescaled by

a factor four and replicated twice in the rate domain (see Figure 3.5 when $a = 0$ and compare it with Figure 2.5 when $a = 0$), but it will be better explained later.

The autocorrelation of the signal in (3.2) is obtained using (1.19), (1.23) and (1.24) with $M = 2$ and it is given by:

$$R_{e_s}(r) = 2\mathrm{R}_{e_p}(\mathrm{r}) - \mathrm{R}_{e_p}(\mathrm{r}-2) - \mathrm{R}_{e_p}(\mathrm{r}+2) \quad (3.3)$$

$$= \frac{1}{8}[\langle(\mathrm{r}-2)\mathrm{s}\rangle(1-\langle(\mathrm{r}-2)\mathrm{s}\rangle) + \langle(\mathrm{r}+2)\mathrm{s}\rangle(1-\langle(\mathrm{r}+2)\mathrm{s}\rangle) - 2\langle\mathrm{rs}\rangle(1-\langle\mathrm{rs}\rangle)] \quad (3.4)$$

Now, in order to obtain the second order IIR digital differentiator, (1.17) and (3.1) have been used to infer the differential equation. The result is given by:

$$v(n) = a[a_1 v(n-1) + a_2 v(n-2)] + (1-a)s(n) \quad (3.5)$$

$$= a[a_1 v(n-1) + a_2 v(n-2)] + \frac{(1-a)}{2}[p(n) - p(n-2)] \quad (3.6)$$

The transfer function derived by (3.6) is given by:

$$H(z) = \frac{1-a}{2} \cdot \frac{1-z^{-2}}{1-aa_1 z^{-1} - aa_2 z^{-2}} \quad (3.7)$$

Comparing (3.5), (3.6) and (3.7) with the equivalent formulae of the first order IIR digital differentiator can be seen why the previous was a kind of special case and it lacked from generality: in the filter of second or higher order the coefficients of the denominator are not fixed and they represents a filter design challenge in the project. In the following section the aspects of this problem will be presented.

3.1.1 Zero-Pole layout

In the differential equations ((3.5) and (3.6)) and in the transfer function (3.7) of the second order IIR digital differentiator, in addition to the feedback coefficient a, there are other two coefficients, labelled with a_1 and a_2, that have to be taken in account during the design of the filter. These additional grades of liberty in the project allow the designer to decide where the two poles have to be placed in the zero-pole layout: in the first order differentiator this choice was already built in. However, since the system must have real coefficients, the poles will be or both in the real axis (the denominator has two real roots) or complex conjugate (the denominator has two complex roots with same real part and opposite imaginary part).

Figure 3.1 shows different zeros-poles layouts for various choices of the feedback coefficient and the other two free coefficients. It can be easily seen from the plot the property that has just been presented regarding real or complex roots of the denominator: in the blue, brown, and green are depicted couple of real poles, while in red and black are depicted the couple of complex conjugate poles. As in the previous chapter, as much higher is the feedback coefficient as much higher is the absolute value of the poles for fixed values of a_1 and a_2. However, in this case the stability of the filter has to be tested with $a = 1$, so it remain valid for every choice of the feedback coefficient.

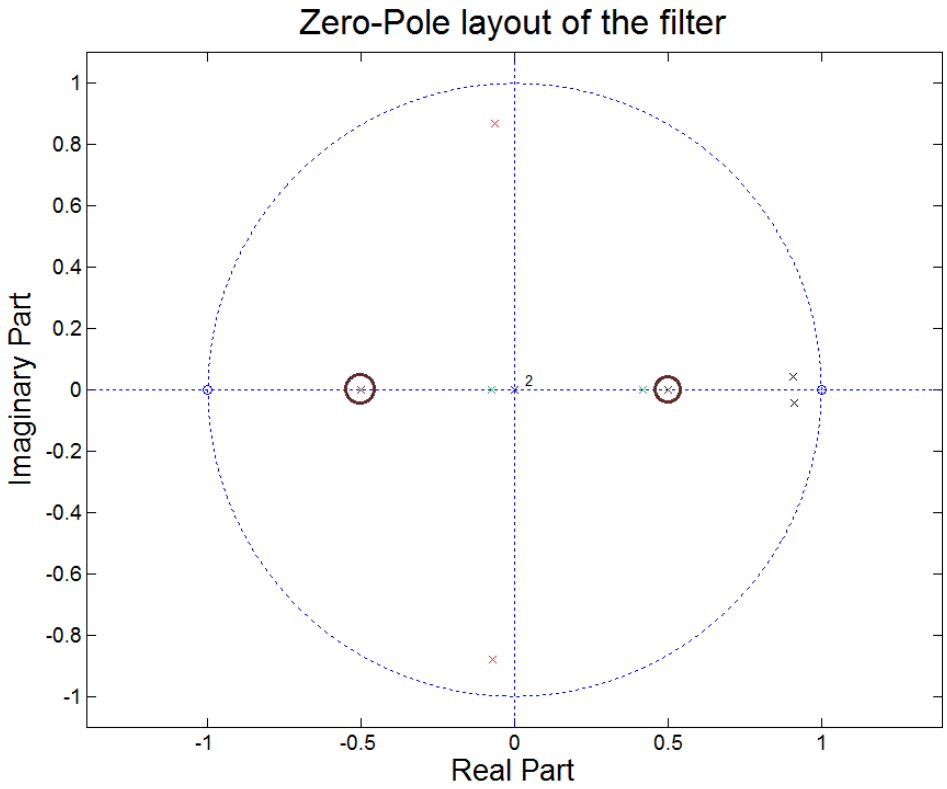

Figure 3.1: Zeros-Poles layout of the second order IIR digital differentiator for different value of the coefficients. The brown poles represent one of the best choice for the filter coefficient since they have equal absolute value and same phase angle than the zeros.

Using the function *fdatool* from the DSP toolbox of Matlab, an optimal way to choose the coefficients of the denominator of the filter has been discovered: when the poles have the same phase angle of the respective zeros (in Figure 3.1 are 0 and π), the best noise attenuation is achieved. Moreover, the two poles need to have the same absolute value (which is the reason why the green poles in Figure 3.1 are not optimal) and, closer are the poles to them respective zero, higher is the attenuation of the overall filter.

Another important property, which is consequent of the above coefficients choice, regards the mean square error: it gets evenly decreased, even if there are main lobes higher than others. This feature is very useful because, when the feedback coefficient is big enough, the output MSE is flattened and it could be approximated in a good way by the white noise or even better by the worst case approximations, simplifying possible simulation that does not the exact value of the MSE.

In the particular case of the second order IIR digital differentiator the optimal choices for the two coefficients of the denominator are $a_1 = 0$ and $a_2 = -1$. When $a = 0$ the poles are in the origin but, increasing the feedback coefficient, the two poles move closer and closer along the x-axis to the respective zeros.

3.1.2 Magnitude, phase and group delay of the differentiator

Using the optimal filter coefficient obtained in section 3.1.1, the new transfer function derived by (3.7) is given by:

$$H(z) = \frac{1-a}{2} \cdot \frac{1-z^{-2}}{1-az^{-2}} \tag{3.8}$$

As in the previous chapter the feedback coefficient plays the role of the trade-off between attenuation of the quantization noise and low overall group delay. The following plots show how.

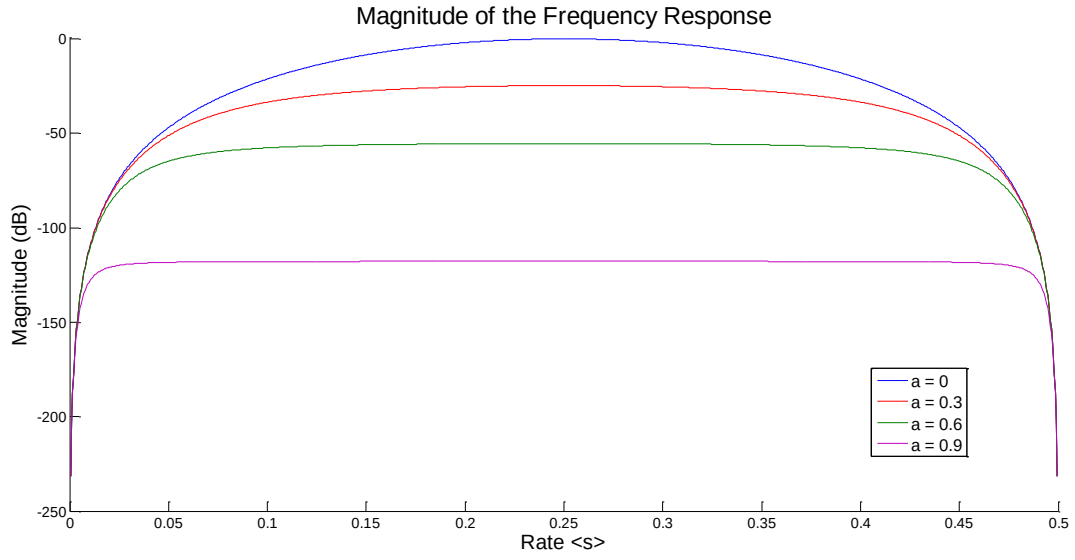

Figure 3.2: Frequency response (on the normalized frequencies) of the second order IIR digital differentiator for various value of the feedback coefficient.

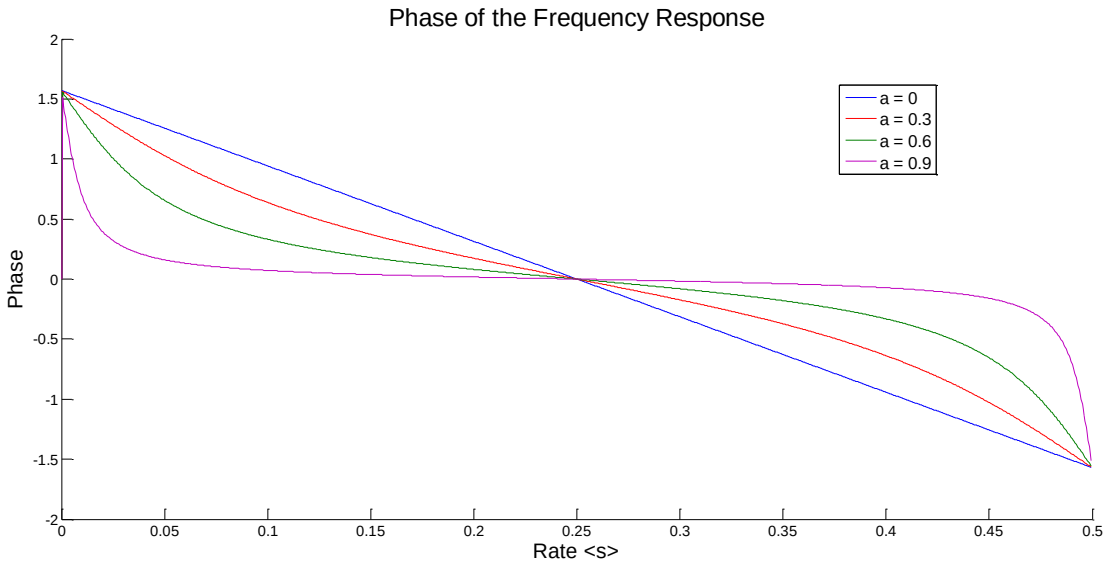

Figure 3.3: Phase of the second order IIR digital differentiator for different value of the feedback coefficient.

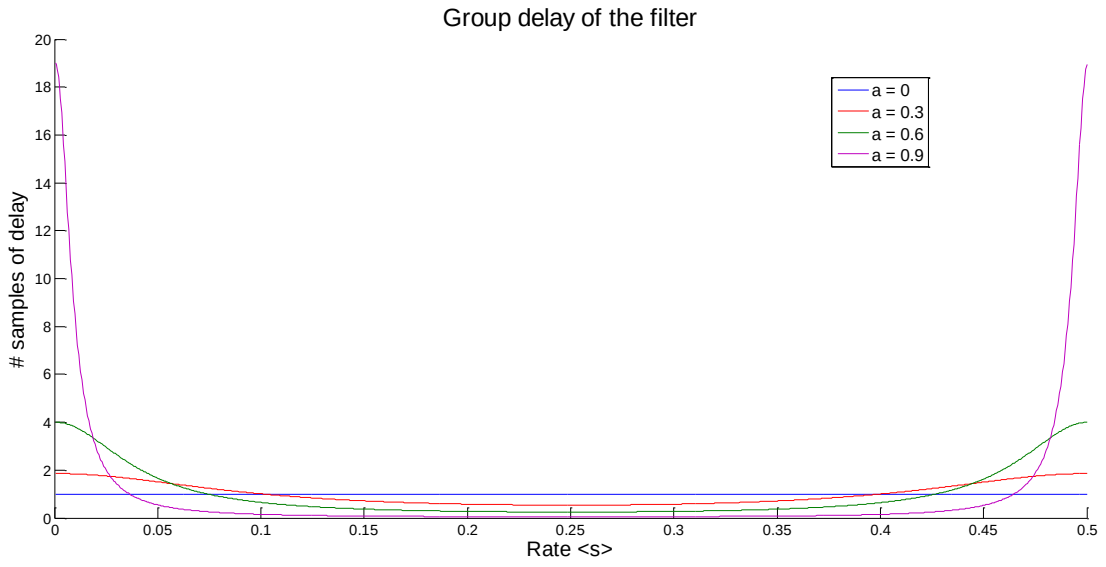

Figure 3.4: Group delay of the second order IIR digital differentiator for different value of the feedback coefficient.

3.2 Quantization mean square error

Using the same method of section 2.2, a closed form solution for the quantization mean square error of the second order IIR digital differentiator will be derived in this section.

The error formula associated to (3.5) is given by:

$$e_v(n) = a[a_1 e_v(n-1) + a_2 e_v(n-2)] + (1-a)e_s(n) \tag{3.9}$$

The first step to obtain the system of equations used to derive $R_{e_v}(0)$ is to multiply (3.9) by $e_v(n), e_v(n-1)$ and $e_v(n-2)$. Then, since $e_v(n)$ and $e_s(n)$ are quasiperiodic and almost stationary signals, they are subjected to the theory in sections 1.2.2 and 1.3 and taking the expectation of the three equations (the outcomes are the autocorrelations and cross-correlation) the resulting system is given:

$$\begin{aligned}
\mathrm{R}_{\mathrm{e_v}}(0) &= \mathrm{a}[a_1 \mathrm{R}_{\mathrm{e_v}}(1) + a_2 \mathrm{R}_{\mathrm{e_v}}(2)] + (1-\mathrm{a})\mathrm{R}_{\mathrm{e_{vs}}}(0) \\
\mathrm{R}_{\mathrm{e_v}}(1) &= \mathrm{a}[a_1 \mathrm{R}_{\mathrm{e_v}}(0) + a_2 \mathrm{R}_{\mathrm{e_v}}(1)] + (1-\mathrm{a})\mathrm{R}_{\mathrm{e_{vs}}}(-1) \\
\mathrm{R}_{\mathrm{e_v}}(2) &= \mathrm{a}[a_1 \mathrm{R}_{\mathrm{e_v}}(1) + a_2 \mathrm{R}_{\mathrm{e_v}}(0)] + (1-\mathrm{a})\mathrm{R}_{\mathrm{e_s}}(-2)
\end{aligned} \tag{3.10}$$

The system in (3.10) is composed by three equations but it has six variables because the close form solutions for $\mathrm{R}_{\mathrm{e_{vs}}}(0)$, $\mathrm{R}_{\mathrm{e_{vs}}}(-1)$ and $\mathrm{R}_{\mathrm{e_{vs}}}(-2)$ are unknown at the moment. Forcing a recursive substitution of the $\mathrm{e_v}(\mathrm{k})$ terms in (3.9) equation (3.11) is derived.

$$\begin{aligned}
&\mathrm{e_v}(n) = (1-a)\sum_{k=0}^{\infty}(aa_1 b_{k-1} + aa_2 b_{k-2})\mathrm{e_s}(n-k) \\
&\text{With initial conditions } b_{-1} = 0, b_{-2} = (aa_2)^{-1} \\
&\text{And recurrence equation } b_i = aa_1 b_{i-1} + aa_2 b_{i-2} \quad \forall i \geq 0
\end{aligned} \tag{3.11}$$

Multiplying both side of (3.11) by $\mathrm{e_s}(n)$, $\mathrm{e_s}(n+1)$ and $\mathrm{e_s}(n+2)$ and then taking the expectation of the resulting outcomes, the last three equations needed are inferred and they are the following (the initial conditions and recurrence equation are the same of (3.11) and $R_{\mathrm{e_s}}(r)$ is given by equations (3.3) or (3.4)):

$$\begin{aligned}
R_{\mathrm{e_{vs}}}(0) &= (1-a)\sum_{k=0}^{\infty}(aa_1 b_{k-1} + aa_2 b_{k-2})R_{\mathrm{e_s}}(k) \\
R_{\mathrm{e_{vs}}}(-1) &= (1-a)\sum_{k=0}^{\infty}(aa_1 b_{k-1} + aa_2 b_{k-2})R_{\mathrm{e_s}}(k+1) \\
R_{\mathrm{e_{vs}}}(-2) &= (1-a)\sum_{k=0}^{\infty}(aa_1 b_{k-1} + aa_2 b_{k-2})R_{\mathrm{e_s}}(k+2)
\end{aligned} \tag{3.12}$$

Solving the system in (3.10) in the variables $\mathrm{R}_{\mathrm{e_v}}(0)$, $\mathrm{R}_{\mathrm{e_v}}(1)$ and $\mathrm{R}_{\mathrm{e_v}}(2)$ and keeping track only for the first of them, the closed form solution for the quantization mean square error is obtained and it is given by:

$$MSE_{e_v} = \mathrm{R}_{\mathrm{e_v}}(0) = \frac{(1-a)\left[(1+aa_2)aa_1R_{vs}(-1) + (1-aa_2)\left(R_{vs}(0) + aa_2R_{vs}(-2)\right)\right]}{(1+aa_2)(1-aa_2+aa_1)(1-aa_2-aa_1)} \quad \textbf{(3.13)}$$

Substituting the terms of (3.12) in (3.13) and then using one of the two between (3.3) and (3.4) a formula with a direct connection between the autocorrelation of the input error $\mathrm{e_p}(n)$ and the autocorrelation of the output error $\mathrm{e_v}(n)$ can be obtained. To remark the importance of the results that have just been presented, can be seen that using equation (3.3) the close form solution of the output MSE is valid for every kind of input whose autocorrelation is known and every kind of second order IIR digital differentiators with optimal filter coefficients in the numerator. Moreover, can be seen that with slightly adjustments in the autocorrelation $\mathrm{R}_{\mathrm{e_s}}(r)$ (to be more precise using general coefficients for the numerator instead of the optimal for the differentiator) the solution obtained is an adaptation of (3.13) and it is valid for every second order IIR filter when the autocorrelation of the input is known.

For the particular purpose of the project, equation (3.4) has been substituted in (3.12) and some Matlab tests have been made in order to verify the correctness of the results when in input there are position information of a constant speed rotating shaft. The comparison between the theoretical expectations and the real outcome perfectly matches (the difference between them is about 10^{-6} and it is reasonably due to rounding and numerical imprecisions in Matlab, so it is negligible). Figure 3.5 shows the plot of the values of the MSE_{e_v} at the output of the filter with optimal coefficients (see section 3.1.1) and can be seen that every rate $\langle s \rangle$ is equally attenuated, without leaving higher spikes in the plot. Every other coefficients configuration presents in the plot of the MSE some spikes higher than others. This choice has two implications: first the results at the output of the IIR differentiator are poorer. Second the worst case approximation leads to worse estimations because, even with high feedback coefficient, theMSE_{e_v} is not flattened.

As for the first order IIR digital differentiators, the feedback coefficient is a trade-off between high noise attenuation and high group delay and it has to be carefully designed in order to match the project specifications.

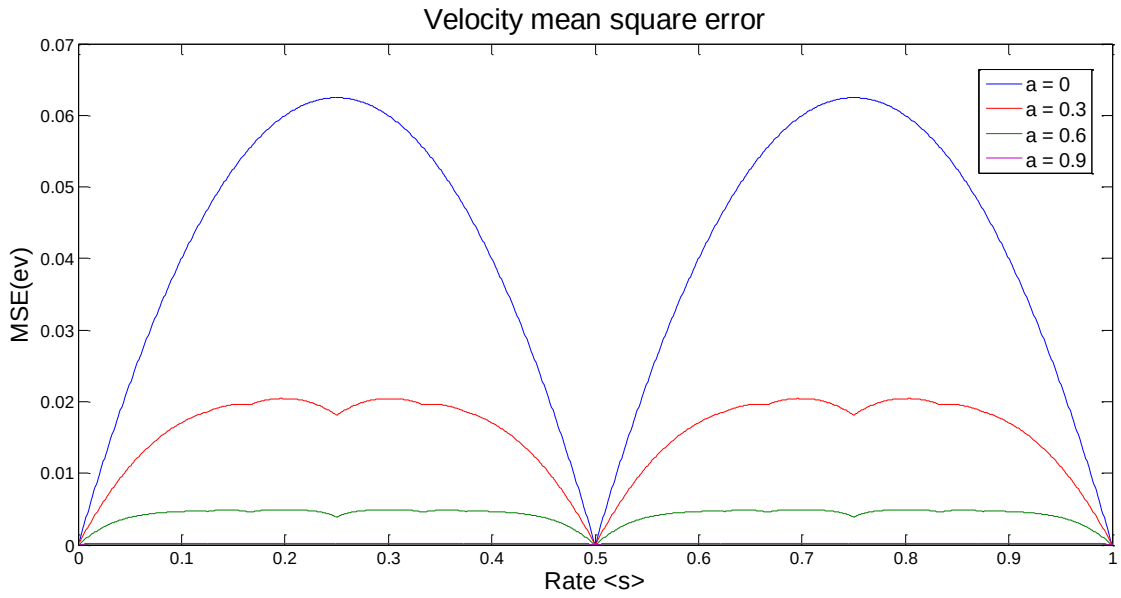

Figure 3.5: Velocity estimation mean square error of the second order IIR digital differentiator for different value of the feedback coefficient.

3.3 Comparison with the white noise assumption

As made for the first order in section 2.3, in this section is going to be presented a closed form solution for the white noise approximation of the quantization mean square error, when the second order IIR digital filter is used.

The inferring process is almost the same used in the previous chapter: using the Åström, Juri and Agniel algorithm (see section 1.2.1) and the coefficients of equation (3.7), a raw formula was derived and then the outcome has been rescaled by the white noise variance (that is 1/12). The result of the process that has just been described is summarized in the following equation:

$$R_{w_v} = \frac{(1-a)^2}{24(1+a)} \tag{3.14}$$

To prove the correctness of equation (3.14), a Matlab function has been developed and it uses equation (2.18) as countercheck of the theoretical results. The experimental and theoretical results matches, confirming that the results obtained so far are correct. The following plots show the comparison between the white noise approximation of the second order IIR digital differentiator and the real shape of the MSE of $e_v(n)$.

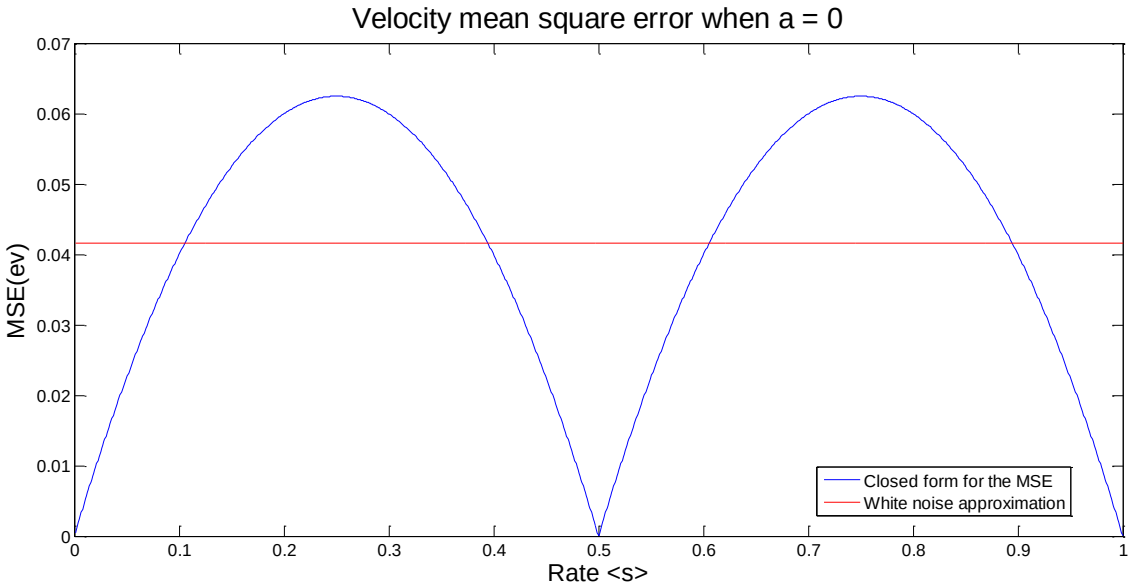

Figure 3.6: Comparison between the output MSE and the white noise approximation when $a = 0$.

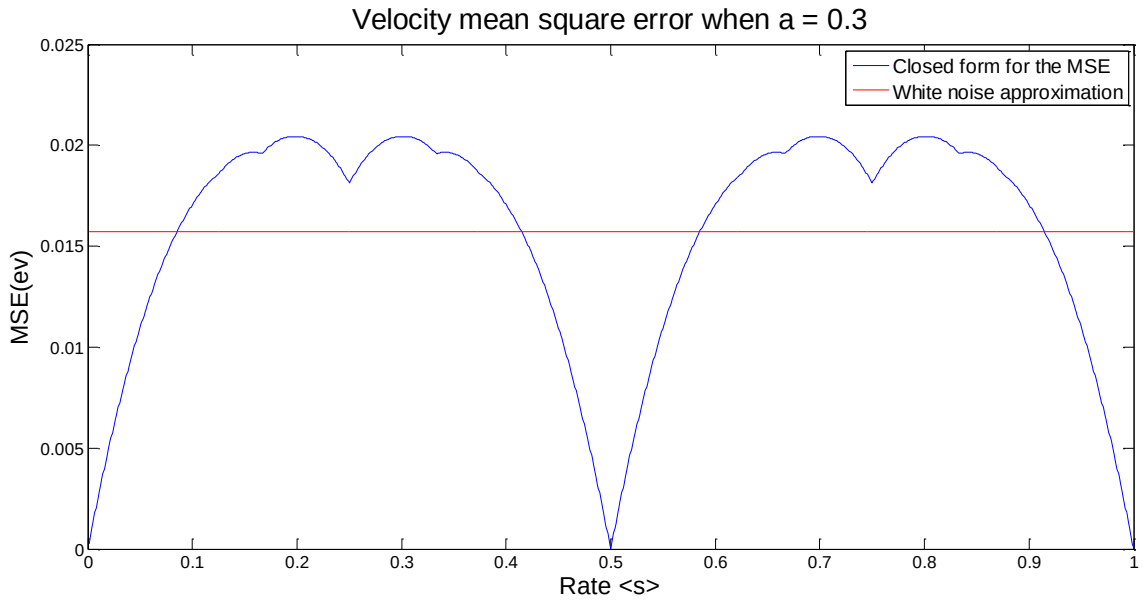

Figure 3.7: Comparison between the output MSE and the white noise approximation when $a = 0.3$.

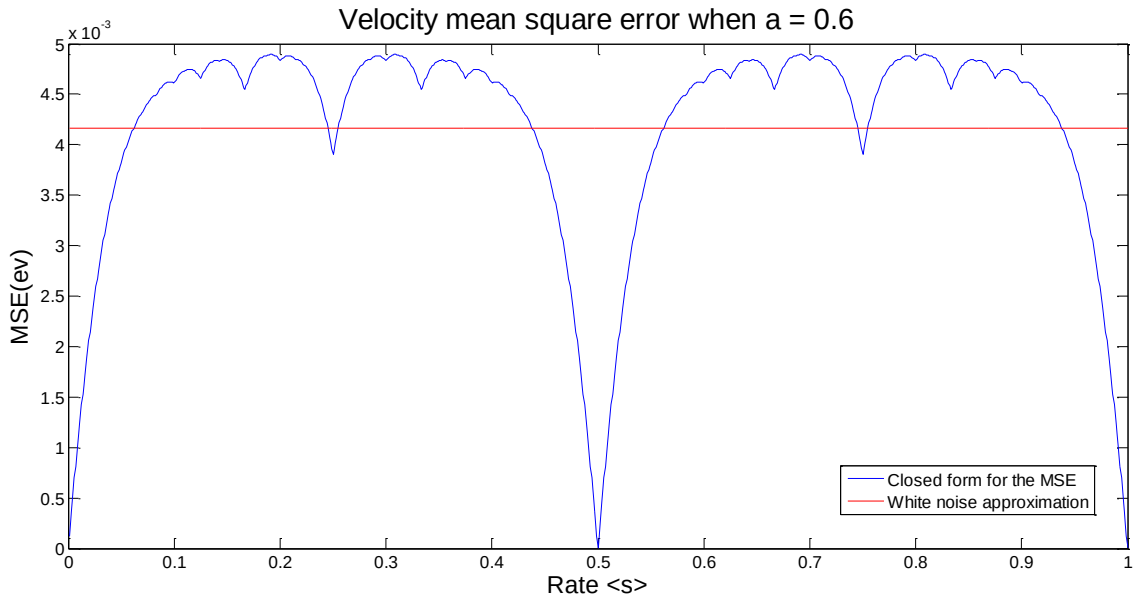

Figure 3.8: Comparison between the output MSE and the white noise approximation when $a = 0.6$.

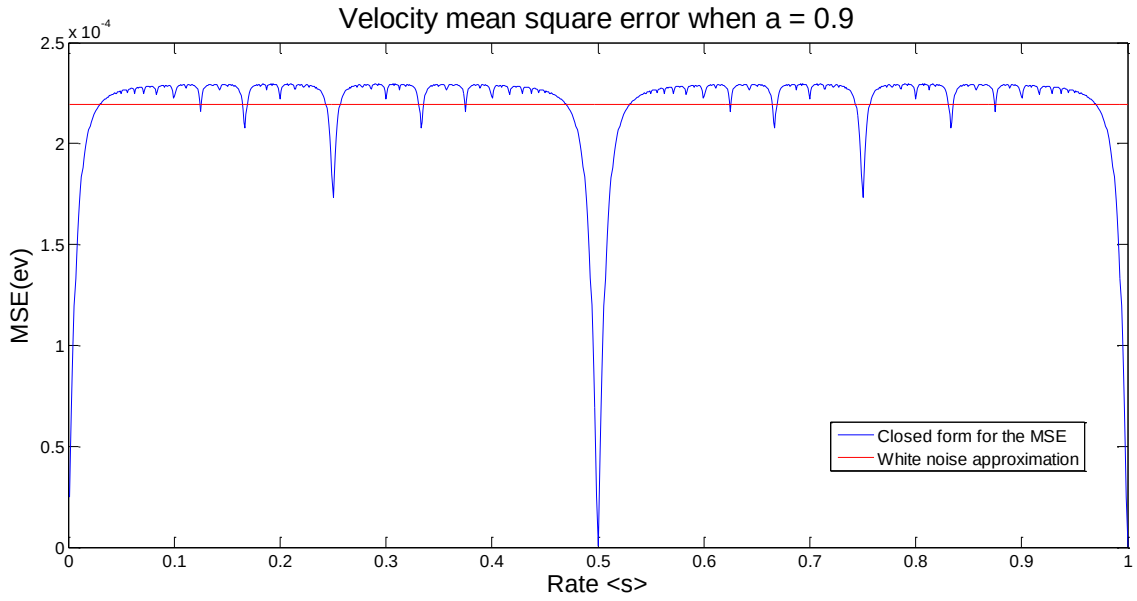

Figure 3.9: Comparison between the output MSE and the white noise approximation when $a = 0.9$.

The comment made on the same section of the previous chapter are valid also for the second order IIR digital differentiator so, the white noise approximation is most of the time poor if applied in digital tachometry. Moreover, it provides an estimation that sometimes is finer than the real MSE, giving no chance to itself to be used as feedback in a close loop control system.

3.4 Worst case approximation

This section has the same motivations and it follows the same assumptions of section 2.4: a worst case approximation of the quantization mean square error is needed when the estimated velocity is used in a close loop control system, because the system must not behave in unexpected or unwanted manner. The optimal coefficients described in section 3.1.1 will be used for the IIR digital differentiator; however, with simple adjustments in the deriving process, it can be used for several filters.

The process used to infer the formula is similar to the one used in the previous chapter and here will be shown only the main points: at the beginning the worst case of the FIR part of the filter is calculated and it is applied to the white noise approximation. If the results of the formula just discovered are not reasonably good, a corrective factor would be inserted in the equation.

The FIR part of the filter has a quantization mean square error at the output that is given by $R_{e_s}(0) = 1/4\,\langle 2s\rangle(1-\langle 2s\rangle)$. Using the mathematical analysis on the variable $\langle 2s\rangle$ can be discovered that the maximum of the function is 0.0625 (on the rates $\langle s\rangle = 0.25$ and $\langle s\rangle = 0.75$). The following formula can be derived using the previous result for rescaling the white noise approximation error:

$$R_{wc_v} = 0.0625\frac{(1-a)^2}{1+a} \tag{3.15}$$

Fortunately, as in the first order, the percentage difference between the worst case of the MSE_{e_v} and the proposed approximation suffers a 3% rate of error with 3% of offset. Splitting equation (3.15) in the cases $a = 0$ and $a \neq 0$, and using the same corrective factor of equation (2.21) when $a \neq 0$, an improved formula can be achieved.

The overall result of the process, which has just been presented, is summarized in the following equation:

$$R_{wc_v} = \begin{cases} 0.0625 & when\ a = 0\ (FIR) \\ 0.0625\dfrac{(1-0.3(a+0.1))(1-a)^2}{1+a} & when\ a \neq 0 \end{cases} \tag{3.16}$$

Experimental proofs on the validity of equation (3.16) have been developed in order to verify its quality. The results are show in the table below:

a	Approximation (3.16)	Real value (3.13)	Percentage difference
0	0.0625	0.0625	0
0.1	0.0432613636363636	0.0429742616876865	0.664
0.2	0.0303333333333333	0.0299184557129206	1.368
0.3	0.0207307692307692	0.0204368290004541	1.418
0.4	0.0136607142857143	0.0134842136612915	1.292
0.5	0.00854166666666667	0.00844816702518876	1.095
0.6	0.00493750000000000	0.00489507855515121	0.859
0.7	0.00251470588235294	0.00249895889340621	0.626
0.8	0.00101388888888889	0.00100948208428638	0.435
0.9	0.000230263157894737	0.000229482965915025	0.339

This approximation, as the previous, has an average difference of 0.81% and worst results occur when a = 0.2, 0.3 and 0.4. However, due to the goodness of the results achieved so far, it has been believed to not investigate any further for a better optimization

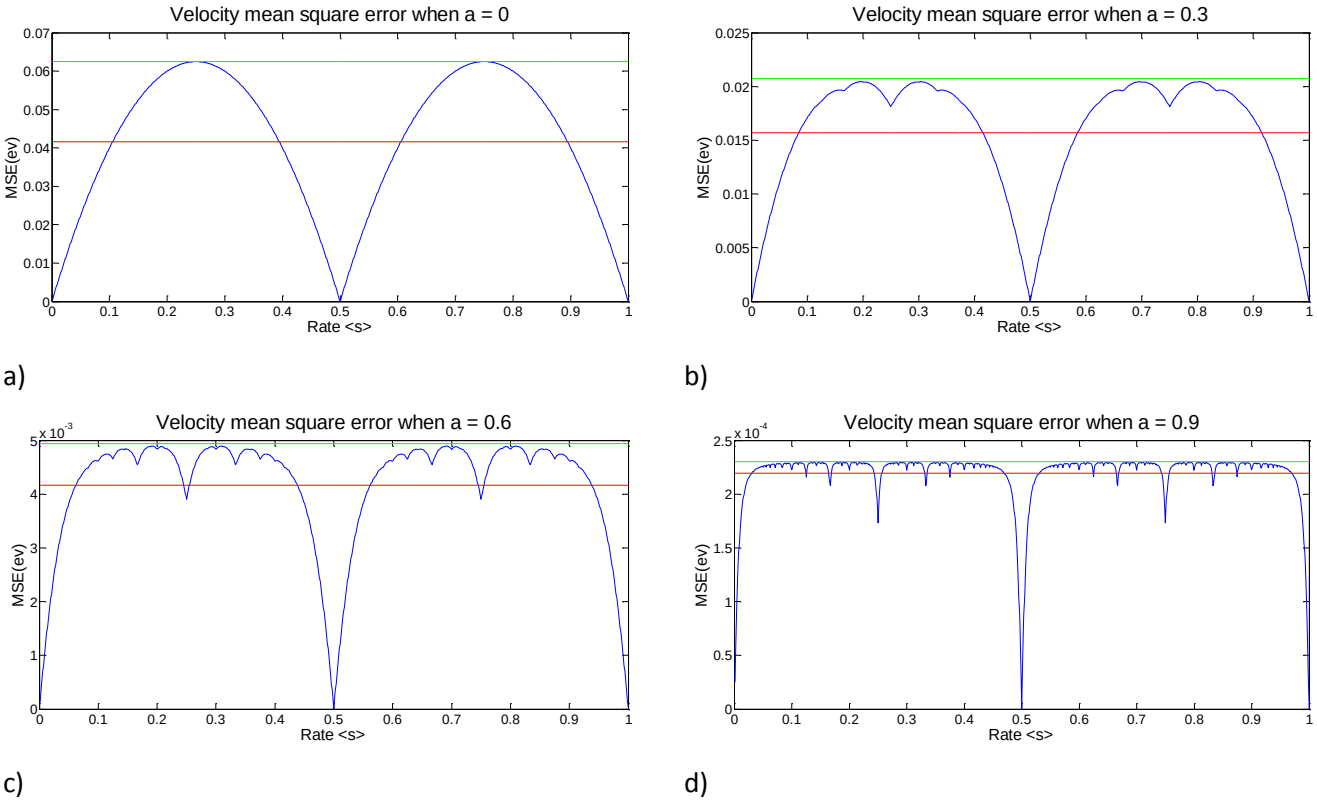

Figure 3.10: Comparison between worst case approximation (green), white noise approximation (red) and real output mean square error (blue) for different values of a: a) $a = 0$, b) $a = 0.3$, c) $a = 0.6$ and d) $a = 0.9$.

3.5 Spectral analysis

The spectral analysis of the second order IIR digital differentiator follows the same steps used in the previous chapter: given the transfer function of the filter (as in equation (3.7)), the frequency response and its magnitude response have been derived. The output power spectrum in obtained by multiplying the magnitude response by the input power spectrum, which again is given by equation (1.25).

The frequency response of the second order IIR digital differentiator is given by:

$$H\left(e^{j\omega}\right) = \frac{1-a}{2} \cdot \frac{1 - e^{-2j\omega}}{1 - aa_1 e^{-j\omega} - aa_2 e^{-2j\omega}} \tag{3.17}$$

Labelling with $r_1 e^{j\theta_1}$ and $r_2 e^{j\theta_2}$ the roots of the polynomial at the denominator of equation (3.17), which are functions of a, a_1 and a_2, the square magnitude response of the filter can be derived as a close form solution. It is given by:

$$\left|H\left(e^{j\omega}\right)\right|^2 = \frac{(1-a)^2}{2} \frac{1 - \cos(2\pi 2ks)}{(1 + {r_1}^2 - 2r_1\ \cos(2\pi ks))(1 + {r_2}^2 - 2r_2\ \cos(2\pi ks))} \tag{3.18}$$

Simply multiplying equation (3.18) by the input power spectrum $P_{e_p}(f)$, the output power spectrum $P_{e_v}(f)$ can be obtained as follow:

$$P_{e_v}(f) = \frac{(1-a)^2}{8\pi^2 \mathrm{k}^2} \frac{1 - \cos(2\pi 2ks)}{(1 + {r_1}^2 - 2r_1\ \cos(2\pi ks))(1 + {r_2}^2 - 2r_2\ \cos(2\pi ks))} \tag{3.19}$$

Using the optimal coefficients of section 3.1.1, which were developed for the constant rate case, equation (3.19) can be rewritten as follow:

$$P_{e_v}(f) = \frac{(1-a)^2}{8\pi^2 \mathrm{k}^2} \frac{1 - \cos(2\pi 2ks)}{1 + a^2 - 2a\cos(2\pi 2ks)} \tag{3.20}$$

In order to prove the correctness of the close form solution of the output power spectrum Figure 3.11 shows the comparison between the theoretical results obtained by (3.20) and the experimental results obtained using large dataset. The difference between the two spectrums is negligible.

Comparing Figure 1.11, Figure 2.11 and 3.11 can be seen how the power spectrum varies only in its magnitude, in the particular situation of constant rate case (in all the three pictures the velocity is $\mathrm{s} = 0.1143$).

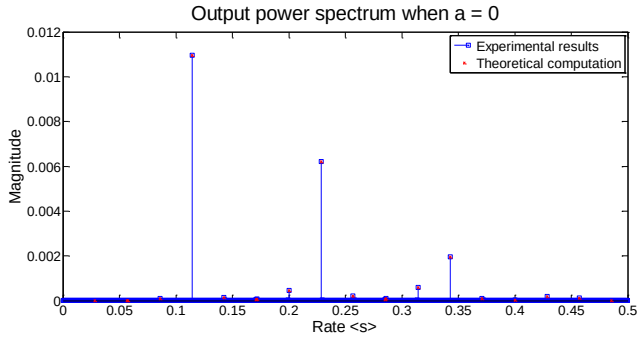

a)

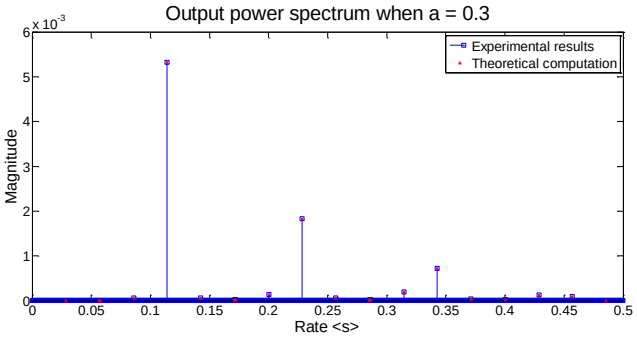

b)

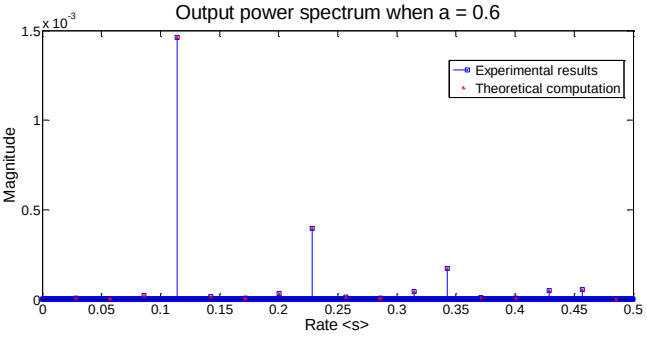

c)

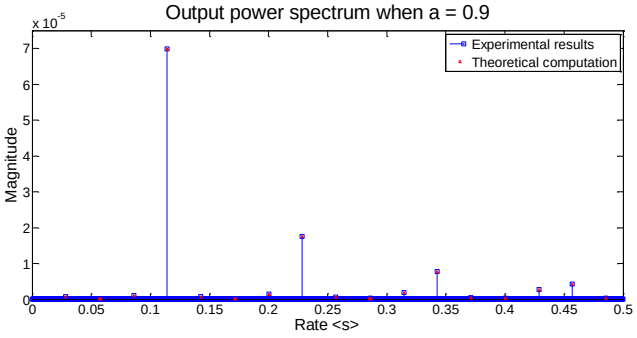

d)

Figure 3.11: Comparison between the theoretical and the experimental results with input rate $s = 0.1143$ and for different values of a: a) $a = 0$, b) $a = 0.3$, c) $a = 0.6$, d) $a = 0.9$

4 General order IIR digital differentiator

The previous two chapters explain the entire framework of the project through two particular cases: the first was mostly focused on the process to achieve all the project's aims with the first order IIR digital differentiator while, the latter, shows some peculiarities that in the first, due to the lack of generality, was missing (e.g. optimal denominator coefficients and linear recurrence equations).

This chapter will provide all the instruments to analyse and design a general order IIR digital differentiator with $M = N$. The most important achievement in the following sections is the pseudo-algorithm that allows everybody to calculate the mean square error at the output of every IIR filter when the autocorrelation of the input is known.

4.1 The filter

The transfer function of the general order IIR digital differentiator has, as numerator, a polynomial with coefficients b_k obtained by (1.15). So, the FIR part of the overall filter, represented by $s(n)$ is given by:

$$s(n) = \sum_{k=0}^{M} b_k p(n-k) \tag{4.1}$$

What is needed now is the autocorrelation $R_{e_s}(r)$, remembering that $e_s(n)$ is the error signal associated to the signal of equation (4.1). It is given by the general case in (1.23) and for the purpose of the thesis by the particular constant rate case in (1.24).

The overall filter is defined by a transfer function, which has the numerator with coefficient of equation (4.1) and a layout as in equation (1.12) or by the differential equation defined in equation (1.17). Equation (1.12) needs to be adjusted in order to insert in it the feedback coefficient. The final result is given as in the following equation:

$$H(z) = \frac{(1-a)\sum_{k=0}^{M} b_k z^{-k}}{1 - \sum_{k=1}^{N} a a_k z^{-k}} \tag{4.2}$$

As explained in the previous chapter the choices for the coefficients a_k are infinite, however, optimal filter coefficient can be obtained as explained in the following section.

4.1.1 Zeros-poles layout

The N zeros of the general order IIR digital differentiator are placed at almost regular intervals in the unity circle of the complex plane every $2\pi/N$ radians starting from $(1,0)$.

In order to achieve the best result in terms of noise attenuation, the N poles must be placed in the same way as zeros, but with absolute value less than the unity. So, every zeros in the form $e^{j\omega}$ (absolute value equal to one and $\omega = 2\pi/i$ with $i \in \{0, \dots, N-1\}$ as phase angle) has an associated pole in $ue^{j\omega}$, where u is the absolute value of the pole. If the poles are complex conjugate will have the same magnitude. Moreover, in order to obtain an even attenuation of the quantization mean square error at the output of the filter at every rates $\langle s \rangle$, all the poles must have the same absolute value. In Figure 4.1 is easy to see what has just been described.

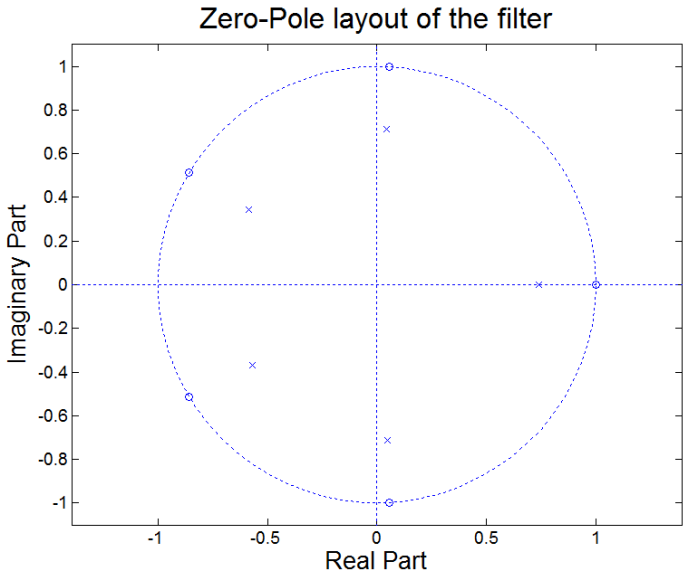

Figure 4.1: Example of a Zeros-Poles layout of the fifth order IIR digital differentiator with aligned couples of pole-zero

In the remainder of the thesis will be referred at such kind of coefficients choice as optimal because no others coefficients reach similar results.

As will be explained in the next section, closer are the poles to the respective zeros, higher is the noise attenuation of the filter. A consequence of this useful property, on the other hand, is that the group delay of the differentiator become spiky in the rates $\langle s \rangle$ which are afflicted by the presence of a zero-pole couple.

4.1.2 Magnitude, phase and group delay of the differentiator

The magnitude, the phase and the group delay of the general order IIR digital differentiator are a generalization of what already seen in sections 2.1.2 and 3.1.2: the zeros of the filter, which are almost equally spaced in the unity circle, provide great attenuation in the nearby rates and a linear phase (or a constant group delay); the poles sensibly increase the attenuation of the filter when they move toward the respective zeros, as can be seen in Figure 4.2. Nevertheless, when the absolute value of the poles are big, the phase of the filter is far from be linear, as depicted in Figure 4.3, and the group delay has spikes in correspondence of the normalized rates which are affected by the presence of a zero-pole couple, easily visible in Figure 4.4.

Figure 4.2 to Figure 4.4 show the particular case of a fifth order IIR differentiator, whose zeros-poles layout is an adaptation to the one depicted in Figure 4.1 for different value of the feedback coefficient.

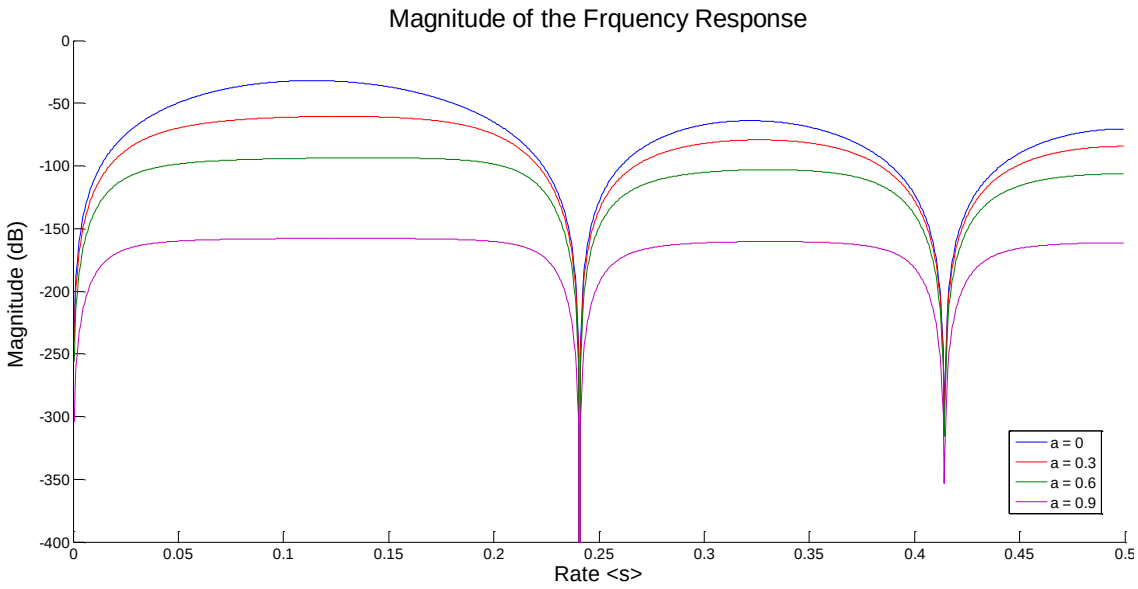

Figure 4.2: Example of magnitude response. In this case M = N = 5.

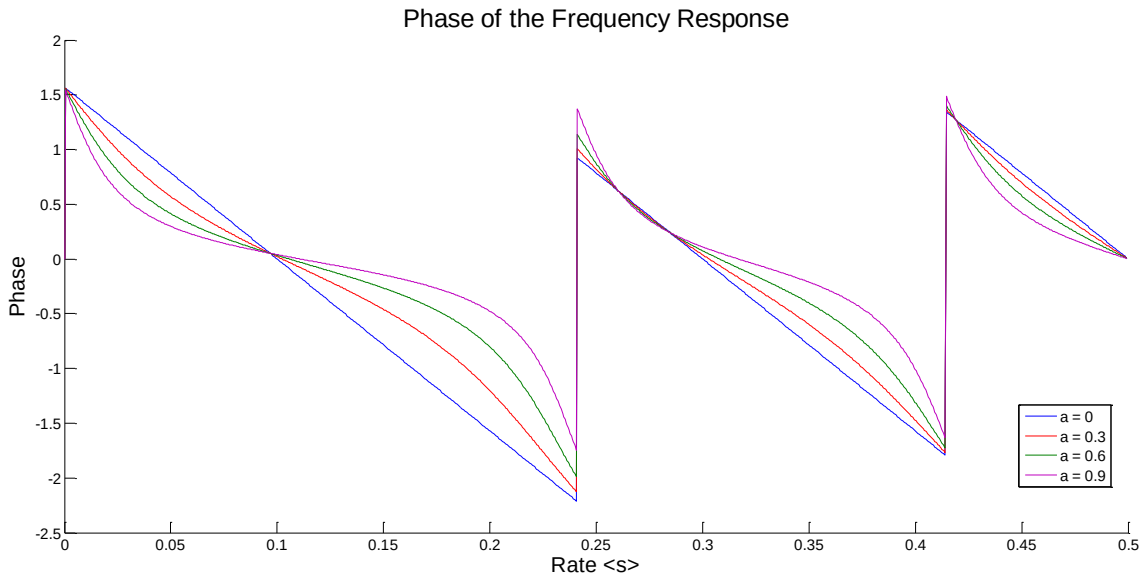

Figure 4.3: Example of phase of the frequency response. In this case M = N = 5.

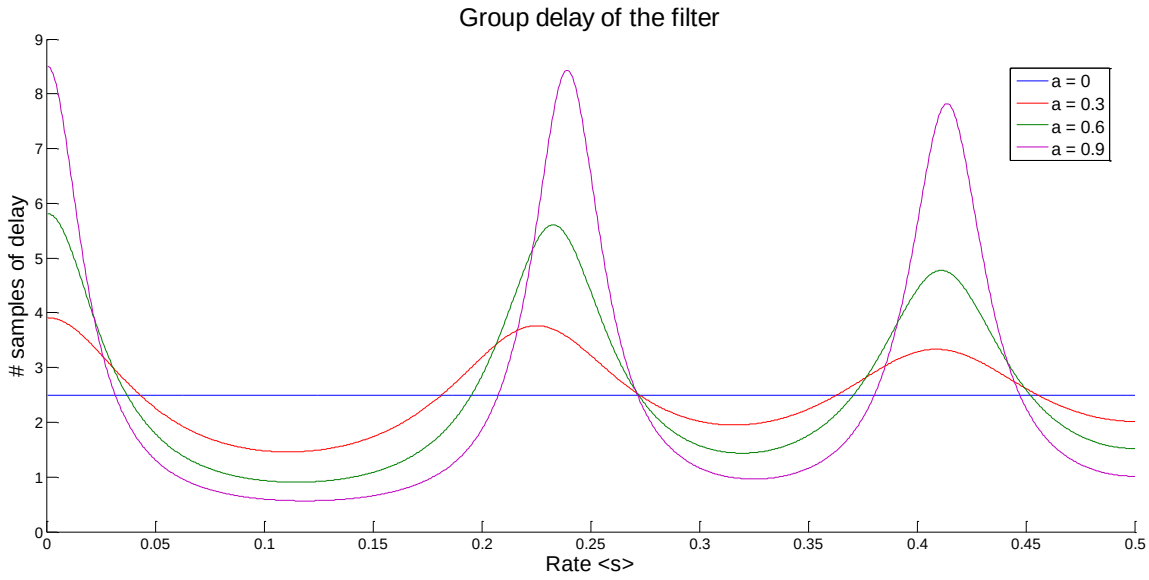

Figure 4.4: Example of group delay of the filter. In this case M = N = 5.

4.2 Quantization mean square error

This section provides a procedure that allows everyone to calculate the quantization means square error at the output of an IIR filter if the autocorrelation of the input error signal, $R_{e_p}(r)$, is known (e.g. the work done so far uses equation (1.19) as autocorrelation of the input error when a rotating shaft with constant velocity is considered).

The IIR differentiator of a general order $M = N$ is given by:

$$v(n) = a\sum_{k=1}^{N} a_k v(n-k) + (1-a)s(n) \quad where \quad s(n) = \sum_{k=0}^{M} b_k p(n-k) \tag{4.3}$$

The error version of the filter associated to equation (4.3) is given by:

$$e_v(n) = a\sum_{k=1}^{N} a_k e_v(n-k) + (1-a)e_s(n) \quad where \quad e_s(n) = \sum_{k=0}^{M} b_k e_p(n-k) \tag{4.4}$$

The first step of the process, in order to calculate a close form solution for the MSE, is to calculate the autocorrelation of the FIR part of the filter, which is held by the signal $e_s(n)$. The results for the general case are shown in equation (1.23) and for the digital tachometer in the constant rate case by equation (1.24).

The successive step is to recursively substitute each $e_v(n-k)$ in the right side of equation (4.4) in order to obtain a direct dependence between the overall output error, $e_v(n)$, and the error at the output of the FIR part, $e_s(n)$.

Using the theory of the linear recurrence equations a general close form solution, which achieves this result, has been derived. It is given by:

$$\mathrm{e_v}(n) = (1-a)\sum_{k=0}^{\infty}(aa_1 b_{k-1} + \cdots + aa_{k-M}b_{k-M})\mathrm{e_s}(n-k)$$
$$\text{With initial conditions } b_{-1} = \cdots = b_{-M+1} = 0, b_{-M} = (aa_M)^{-1} \tag{4.5}$$
$$\text{And recurrence equation } b_i = \textstyle\sum_{j=1}^{M} aa_j b_{i-j} \quad \forall i \geq 0$$

Multiplying both side of (4.5) by $\mathrm{e_s}(n-r)$ and taking the expectations, a formula for the cross-correlation between $\mathrm{e_v}(n)$ and $\mathrm{e_s}(n)$ can be derived and the result is summarized by the following equation:

$$R_{\mathrm{e_{vs}}}(r) = (1-a)\sum_{k=0}^{\infty}(aa_1 b_{k-1} + \cdots + aa_{k-M}b_{k-M})R_{\mathrm{e_s}}(r-k)$$
$$\text{With initial conditions } b_{-1} = \cdots = b_{-M+1} = 0, b_{-M} = (aa_M)^{-1} \tag{4.6}$$
$$\text{And recurrence equation } b_i = \textstyle\sum_{j=1}^{M} aa_j b_{i-j} \quad \forall i \geq 0$$

In order to achieve $MSE_{\mathrm{e_v}}$, which can be calculated as $R_{\mathrm{e_v}}(0)$, the next step is the following: multiply both sides of (4.4) by $\mathrm{e_v}(n-i)$ with $\mathrm{i} \in \{0, \ldots, \mathrm{N}\}$, and then taking the expectation

of it, a system with $N+1$ equations in $N+1$ variables, labelled $R_{e_v}(i)$ with i $\in \{0, \dots, N\}$, is eventually obtained.

The final step consists in solving the system of equations that has just been derived, taking in account only the result for $R_{e_v}(0)$ and substituting in it every occurrence of $R_{e_{vs}}(r)$ or $R_{e_s}(r)$ with the results from (4.6) and (1.23). The outcome is the close form solution for the MSE_{e_v} of a general order IIR digital differentiator.

Some simulation has been made in Matlab in order to prove the correctness of the process that has just been proposed. The experimental results perfectly match the theoretical expectations, which have been calculated following the instructions of this section. The importance of this result can be explained by complexity computation because when the mean square error at the output of a filter is needed there are two possible solutions: or some simulations have to be made or a close form solution has to be inferred. The first case requires a small time of setup but, probably, it will need a long time to run (according to the dimension of the input); moreover, the results are bond to the specific type input signal. The latter needs much more time to be developed. However, it offers a quick solution in the future, even with different filters or input signals.

The process just explained works for every kind of IIR filter (not only for differentiators and even with $N \neq M$). The only requirement is that the autocorrelation of the input error is known. The flexibility of the algorithm just proposed can be very helpful in the DSP field.

The overall process that has been described in this section of the thesis can be summarized with the following pseudo-code:

Input: $R_{e_p}(r)$: autocorrelation of the input error signal
Differential equation of the filter as in (4.4)

Process:
- Calculate the autocorrelation of the error at the output of the FIR part of the filter: $R_{e_s}(r)$;
- Calculate the cross-correlation $R_{e_{vs}}(r)$ using the formula for the linear recurrence equations;
- Build the equations system in the variables $R_{e_v}(i)$ with i $\in \{0, \dots, N\}$ starting from (4.4);
- Solve the system and obtain $R_{e_v}(0)$
- Substitute in the $R_{e_v}(0)$ every occurrence of $R_{e_{vs}}(r)$ and $R_{e_s}(r)$ with the quantity just obtained

Output: $MSE_{e_v} = R_{e_v}(0)$: Close form solution for the mean square error at the output of the filter

4.3 Comparison with the white noise assumption

As seen in section 2.3 and 3.3, the white noise assumption leads to poor results when used to describe the quantization mean square error when a digital tachometer is used for estimating the velocity of a rotating shaft in the constant rate case. These results remain valid also for IIR digital differentiator with order higher than two: in all these cases, an exception can be made when the value of the feedback coefficient is sufficient high and the MSE_{e_v} is almost flat.

However, the close form solution for the white noise approximation has been derived for the third (4.7) and fourth (4.8) order IIR digital differentiator. Here will be presented only the results but the procedure used to derive them was the same used in section 2.3 and 3.3 using the Åström, Juri and Agniel algorithm (see section 1.2.1).

$$R_{w_v} = \frac{(1-a)^2\left[10 + 9a^2a_2^2 - 3aa_2\left(5 + 3aa_3\right) - aa_4 - 9a^2a_4^2 + aa_3\left(6 + 9aa_4\right)\right]}{600(1 + aa_2 - aa_3 + aa_4)(1 + aa_3 + a^2a_2a_4 - a^2a_4^2)} \tag{4.7}$$

$$R_{w_v} = \frac{(1-a)^2\left[5 + 4a^2a_2^2 + 4aa_2\left(1 - aa_4\right) - 4aa_4 + aa_5 - 4a^2a_5^2 + 4aa_3\left(1 + aa_5\right)\right]}{600\left(1 - a^2a_4^2 + a^2a_2\,a_4\left(1 - aa_5\right) + aa_5 + a^3a_2^2a_5 - a^2a_5^2 - a^3a_5^3 + aa_3\left(1 + aa_5\right)^2\right)} \tag{4.8}$$

As can be seen in (4.7) and (4.8) a close form solution became difficult to manage when the filter has order higher than four and, since it does not provide good results, it was not necessary to investigate any further.

4.4 Worst case approximation

The worst case approximation could lead to results that are more pessimistic than the white noise approximation (see Figure 2.10 and Figure 3.10). However, it can be used in close loop control system without any affection in the stability of the overall system, giving to it particular relevance if compared with the white noise approximation.

Particular attention must be paid when this instrument is used as velocity estimation in a feedback loop: although this noise approximation performs well when the feedback coefficient is high, it does not take in account the group delay that is introduced by the filter. Since this aspect is fundamental in close loop control system, it should be modelled in parallel with the worst case approximation.

Due to the lack of time, the close form solutions for the worst case approximation have been derived only for the first two orders of the IIR digital differentiator. Could be interesting, in a future work, discover an approximation for at least the first five orders of such filters, so a complete framework will be provided to the user.

As seen in the previous chapter, rescaling the white noise approximation with the worst case of the MSE when $a = 0$ and then adding a corrective factor could give interesting results. However, there are not validations on the rightness of the method just proposed or on the quality of the outcomes that it would give.

4.5 Spectral analysis

The spectral analysis of the first two order IIR digital differentiator has been provided in sections 2.5 and 3.5. In these cases a close form solution was achieved.

Due to the complexity of handling higher order differentiator, the general order spectral analysis has been developed with Matlab test cases. As in the previous sections, the input power spectrum $P_{e_p}(f)$ used is the one given by equation (1.25) and the magnitude response of the filter $\left|H\left(e^{jw}\right)\right|^2$ is calculated via the *freqz* function of Matlab. Then the output power spectrum is obtained multiplying these two quantities. The general formula is given by:

$$P_{e_v}(f) = P_{e_p}(f) \cdot \left|H\left(e^{jw}\right)\right|^2 \tag{4.9}$$

The experimental results, obtained with large dataset, were compared with the first 20 components of the input spectrum ($k \in \{1, \dots, 20\}$ in the equation (1.25)) multiplied by the magnitude response of the filter. The outcomes of these tests perfectly match the expectations for filter with order higher than two. Since no strange behaviours were shown in the plots, no further investigation was made in this direction.

5 Future works

The initial aims of the project were the analysis and the design of IIR digital differentiators for quantized signals and the implementation of that knowledge on a physical digital tachometer. Since the results from the analysis of the filters gave lots and very good results, it has been decided to continue in a deeper and wider analysis rather than beginning also an implementation of the project. This decision leaves the entire implementation as future work: further proofs of the rightness of the results achieved so far can be obtained experimentally, implementing all the theory developed in this thesis with an incremental optical encoder and a DSP board.

Another important project, which could be a spinoff of this work, should be a comparison between FIR and IIR digital differentiator: it can be based on the lowest quantization mean square error achievable, linearity of the group delay or a balance between these two aspects. This work could give a more clear idea on how much better the IIR filters perform compared to the FIR and how big is the ratio between the orders of an FIR and an IIR differentiators that achieve the same results.

When a filter is needed in a close loop control system that involve only constant group delay, the FIR differentiators could be favoured, due to their constant group delay; however, a complete survey on the use of equalizer, in cascade to the IIR differentiator, could give more information on the choice between a higher orders FIR rather than a low order IIR with an equalizer in cascade.

Another important project could be based on noisy input signal in fact in this thesis the only error in the system were introduced by the quantizer. Especially in the constant rate case, which was largely discussed in this thesis, if the input signal is affected by some kind of noise, in addition to the quantization noise, it does not mean that the results are worse: the additive error could relax the strong correlation between signal samples, making the analysis easier and, maybe, more useful the white noise approximation. In this direction could be developed a research on an additive dithering signal, which are largely used with quantized signals.

Last, a more theoretical aspect could be to derive the closed form solution for the white noise approximation and the worst case approximation for IIR differentiator with order higher than those derived in this thesis. Adding the results of this work in this thesis would offer a complete survey on the IIR digital differentiator of a considerable order.

Conclusions

The work done so far presents a procedure that allows everybody to calculate the mean square error at the output of an IIR filter, when the autocorrelation of the input error signal is known. This achievement has general meaning and can be applied in different fields of DSP. More specifically, when the input is provided by an incremental optical encoder, a complete discussion on the constant rate case has been done.

Another achievement concerns the comparison between the real MSE and the two approximations: white noise and worst case. While the first noise estimation is useless in digital tachometry (except when the feedback coefficient is big enough), the second provides an interesting and easy tool, especially when the estimated velocity is used in a close loop control system.

The innovation introduced by this project in the digital signal processing filed makes it eligible for a publication. An attempt, in this direction, will be made in the near future with the collaboration of Prof. Richard Kavanagh.

A comment about the comparison between FIR and IIR filters can be made, even if no formal counterproof has been developed. In [12] a 16 order FIR differentiator is presented, which achieves worse results than the first order IIR digital differentiator: this means that when the filter is used in digital tachometry only for the sake of velocity estimation (such as in an open loop control system), a great reduction of the order of the filter used can be achieved, saving time and efforts.

Relevant literature

[1] R. C. Kavanagh, "Improved analysis and design techniques for digital tachometry", Ph. D. Thesis, July 1998.

[2] W. R. Bennett, "Spectra of Quantized Signals", *Bell System Technical Journal*, Vol. 27, pp. 446-472, July 1948

[3] M. F. Wagdy, "Validity of Uniform Quantization Error Model for Sinusoidal Signals Without and With Dither", *IEEE Transactions on Instrumentation and Measurement*, Vol. 38, No. 3, pp. 718-722, June 1989

[4] R. M. Gray, "Quantization noise spectra", *IEEE Transactions on Information Theory*, Vol. 36, No. 6, pp. 1220-1244, November 1990

[5] H. B. Kushner, M. Meisner, A. V. Levy, "Almost Uniformity of Quantization Errors", *IEEE Transactions on Instrumentation and Measurement*, Vol. 40, No. 4, pp. 682-687, August 1991

[6] Robert M. Gray, T. G. Stockham, "Dithered Quantizers", *IEEE Transactions on Information Theory*, Vol. 39, No. 3, pp. 805-812, May 1993

[7] T. P. Borsodi, B. Nowrouzian, "Closed-Form Solution of Granular Quantization Error for a Class of Sigma-Delta Modulators", *IEEE International Symposium on Circuit and System*, pp. 629-632, 1995

[8] B. Widrow, I. Kollar, M-C. Liu, "Statistical Theory of Quantization", *IEEE Transactions on Instrumentation and Measurement*, Vol. 45, No. 2, pp. 353-361, April 1996

[9] R. M. Gray, D. L. Neuhoff, "Quantization", *IEEE Transaction on Information Theory*, Vol. 44, No 6, pp. 2325-2383, October 1998

[10] R. C. Kavanagh, J. M. D. Murphy, "The Effects of Quantization Noise and Sensor Nonideality on Digital Differentiator-Based Rate Measurement", *IEEE Transaction on Instrumentation and Measurement*, Vol.47, No. 6, pp. 1457-1463, December 1998

[11] S. Samadi, M. Omair Ahmad, M. N. S. Swamy, "Z-Transform of Quantized Ramp Signal", *IEEE Transactions on Signal Processing*, Vol.53, No. 1, pp. 380-383, January 2005

[12] R. C. Kavanagh, "FIR differentiator for quantized signals", *IEEE Transaction on Signal Processing*, Vol. 49, No. 11, pp. 2713-2720, November 2001

[13] B. Kumar, C. Dutta Roy, "Design of Digital Differentiators for Low Frequencies", *Proceeding of the IEEE*, Vol. 76, No. 3, pp. 287-289, March 1988

[14] I. W. Selesnick, "Maximally Flat Low-Pass Digital Differentiators", *IEEE Transactions on Circuits and Systems-II: Analog and Digital Signal Processing*, Vol. 49, No. 3, pp. 219-223, March 2002

[15] X. Zhang, T. Yoshikawa, "Design of Full Band IIR Digital Differentiators", *Proceeding of the 2003 International Conference on Neural Network and Signal Processing*, Vol. 1, pp. 652-655, December 2003

[16] M. A. Al-Alaoui, "Linear Phase Low-Pass IIR Digital Differentiators", *IEEE Transactions on Signal Processing*, Vol. 55, No. 2, pp. 697-706, February 2007

[17] A. Tahmasbi, S. B. Shokohui, "New Optimized IIR Low-Pass Filter Differentiators", *International Conference on Signal Acquisition and Processing*, pp. 205-209, 2010

[18] A. J. Koivo, "Quantization Error and Design of Digital Control System", *IEEE Transactions on Automatic Control*, Vol. 14, No. 1, pp. 55-58, 1969

[19] R. D. Lorenz, K. W. Van Patten, "High-Resolution Velocity Estimation for All-Digital, ac Servo Drives", *IEEE Transactions on Industry Applications*, Vol. 27, No. 4, pp. 701-705, July-August 1991

[20] P. J. Roche, J. M. D. Murphy, M. G. Egan, "Reduction of Quantisation Noise in Position Servosystems", *Proceedings of the 1992 International Conference on Industrial Electronics, Control, Instrumentation and Automation*, Vol. 1, pp. 464-469, 1992

[21] R. C. Kavanagh, "Improved Digital Tachometer With Reduced Sensitivity to Sensor Nonideality", *IEEE Transactions on Industrial Electronics*, Vol. 47, No. 4, pp. 890-897, August 2000

[22] R. C. Kavanagh, "Signal Processing Techniques for Improved Digital Tachometry", *IEEE International Symposium on Industrial Electronics*, Vol.2, pp. 511-517, 2002.

[23] S. J. Park, R. M. Gray, "Sigma-Delta Modulation with Leaky Integration and Constant Input", *IEEE Transactions on Information Theory*, Vol. 38, No. 4, pp. 1512-1533, September 1992

[24] L. Ljung, System Identification: Theory for the User, 1st Edition, Prentice Hall, Englewood Cliffs, New Jersey, 1987, Ch. 2.

[25] S. K. Mitra, Digital Signal Processing: a Computer Based Approach, 3rd Edition, McGraw-Hill, 2005.

[26] H. Bohr, Almost Periodic Function, Chelsea Publishing Company, 1947. Translated from the German: Published by Julius Springer, Berlin, 1933